



UNITED NATIONS EDUCATIONAL, SCIENTIFIC AND CULTURAL ORGANIZATION
INTERNATIONAL ATOMIC ENERGY AGENCY
INTERNATIONAL CENTRE FOR THEORETICAL PHYSICS
I.C.T.P., P.O. BOX 586, 34100 TRIESTE, ITALY, CABLE: CENTRATOM TRIESTE



SMR.998a - 3

Research Workshop on Condensed Matter Physics
30 June - 22 August 1997
MINIWORKSHOP ON
QUANTUM MONTE CARLO SIMULATIONS OF LIQUIDS AND SOLIDS
30 JUNE - 11 JULY 1997
and
CONFERENCE ON
QUANTUM SOLIDS AND POLARIZED SYSTEMS
3 - 5 JULY 1997

"Phase Equilibrium in a Polarized Saturated ^3He - ^4He Mixture"

Gerard VERMEULEN
C.N.R.S.
Centre de Recherches Sur Les Très Basses Températures
B.P. 166
Grenoble CEDEX 9 F-38042
FRANCE

These are preliminary lecture notes, intended only for distribution to participants.

MAIN BUILDING STRADA COSTIERA, 11 TEL. 2240111 TELEFAX 224163 TELEX 460392 ADRIATICO GUEST HOUSE VIA GRIGNANO, 9 TEL. 224241 TELEFAX 224531 TELEX 460449
MICROPROCESSOR LAB. VIA BEIRUT, 31 TEL. 2249911 TELEFAX 224600 TELEX 460392 GALILEO GUEST HOUSE VIA BEIRUT, 7 TEL. 2240311 TELEFAX 2240310 TELEX 460392

I don't like the
capitals in the figure
captions

Phase Equilibrium in a Polarized Saturated ^3He - ^4He Mixture

Alexandre Rodrigues* and Gerard Vermeulen

Centre de Recherches sur les Très Basses Températures, laboratoire associé à
l'Université Joseph Fourier, CNRS, BP 166, Grenoble Cédex 9, France

X

(Received July 30, 1996; revised January 27, 1997)

We present experimental results on the phase equilibrium of a saturated ^3He - ^4He mixture, which has been cooled to a temperature of 10–15 mK and polarized in a ^4He circulating dilution refrigerator to a stationary polarization of 15%, 7 times higher than the equilibrium polarization in the external field of 7 T. The pressure dependence of the polarization enhancement in the refrigerator shows that the molar susceptibilities of the concentrated and dilute phase of a saturated ^3He - ^4He mixture are equal at $p = 2.60 \pm 0.04$ bar. This result affects the Fermi liquid parameters of the dilute phase. The osmotic pressure in the dilute phase has been measured as a function of the polarization of the coexisting concentrated phase up to 15%. We find that the osmotic pressure at low polarization (< 7%) agrees well with thermodynamics using the new Fermi liquid parameters of the dilute phase.

1. INTRODUCTION

An unresolved problem in condensed matter physics is the origin of the enhancement of the low field susceptibility of degenerate liquid ^3He , χ_{30} , with respect to the susceptibility of a Fermi gas with the same density, χ_F . Two physical pictures to explain this enhancement have been proposed. The "nearly ferromagnetic" model views liquid ^3He as getting increasingly closer to a ferromagnetic instability with increasing pressure. The large susceptibility is explained as a Stoner enhancement ~~$\chi_{30} = \chi_F / (1 - I\chi_F)$~~ , where $1/(1 - I\chi_F)$ increases from 9.2 to 24 as the pressure increases from 0 to 34 bar.¹ Because the liquid is close to a ferromagnetic instability, critical spin fluctuations ("paramagnons") have to be taken into account. The theory has been successful in describing the low temperature susceptibility,

$$\chi_{30} = \chi_F / (1 - I\chi_F)$$

*Present address: Departamento de Física, Universidade Federal de Pernambuco, Cidade Universitária, 50670901 Recife, PE Brasil.

accounts not very well for the pressure dependence of the effective mass and fails to explain the compressibility. This model predicts an increase of the nuclear polarization, P , with increasing magnetic field, B , slower than obtained by an extrapolation of the low field behavior of $P(B)$.

The "nearly solid" model views liquid ^3He as becoming more and more localized with increasing pressure because of the increasing importance of the hard core repulsive interactions. This approach may be modeled by a lattice-gas with an on-site repulsive interaction: the Hubbard model. A solution of the Hubbard model, using the Gutzwiller approximation accounts rather well for the pressure dependence of the effective mass, compressibility and susceptibility.² It also predicts a meta-magnetic transition, i.e. a magnetization jump in a finite magnetic field. However, the agreement between this model and the susceptibility data is an artifact of the Gutzwiller approximation.³ A more sophisticated description, adding a nearest neighbor ferromagnetic exchange to the Hubbard model gives a more satisfying picture of liquid ^3He .³

Despite the enhancement of susceptibility, it is impossible to obtain highly polarized liquid by brute force in equilibrium ($P = 6.4\%$ in $B = 20$ T at $p = 10$ bar). Therefore, out of equilibrium methods have been developed. In this paper, we use dilution of ^3He as a nuclear orientation technique to study the polarization dependence of the equilibrium between the dilute and concentrated (nearly pure) phase, $^3\text{He}_d$ and $^3\text{He}_c$, of a saturated ^3He - ^4He mixture. The aim of our experiments is to obtain information on the field dependence of the polarization of the concentrated and the dilute phase, $P_{3c}(B)$ and $P_{3d}(B)$.

For almost 15 years the only methods to produce liquid ^3He with a high nuclear spin polarization have been the rapid melting of solid, polarized in a high magnetic field at low temperatures⁴ and the rapid condensation of optically polarized gas.⁵ A disadvantage of both methods is that the polarization relaxes to its equilibrium value. The relaxation time, T_1 , is typically 300s after a rapid condensation⁶ and varies from 10 to 3000 s after a rapid melting (depending on the final temperature and the presence of surface relaxation).^{7,8} While the polarization relaxes, the thermodynamic and transport properties can be studied if all time constants for thermodynamic equilibrium (spin and thermal diffusion time, τ_s and τ_t) are short with respect to T_1 . Experiments have to be designed very carefully to eliminate or control temperature and polarization gradients. For example, polarized liquid ^3He has been produced inside a silver sinter to measure the heat release due to relaxation.⁸ In this experiment, $\tau_s \approx 1$ s and $T_1 \approx 70$ s ~~as~~ and the condition that the polarization changes slowly with respect to the other time constants of the system is fulfilled. The experimental data have been analyzed by means of the second law of thermodynamics to obtain the

polarization as a function of magnetic field for an out of equilibrium polarization up to 60%. The results are in clear disagreement with a meta-magnetic behavior.

During the last five years, new methods to produce liquid ^3He with an out of equilibrium but stationary polarization have been developed. All those methods have in common that the polarization of the sample is the result of a polarization gain due to a circulation of polarized ^3He atoms and a polarization loss due to relaxation:

1. Forced circulation of optically polarized ^3He gas through a ^3He - ^4He liquid mixture.⁹ The experimental setup consists of an U-tube filled with a dilute ^3He - ^4He mixture. One side of the U-tube is heated to evaporate mostly ^3He (the saturated vapor pressure of ^3He is much higher than of ^4He) and the other side is cooled to condense the ^3He . The ^3He gas is forced to flow through a region at room temperature, where it is optically polarized. A polarization of more than 50% at a temperature of about 200 mK has been obtained. Recently, the ^3He inside the dilute mixture has been compressed by means of the heat flush effect and phase separation has been observed.¹⁰
2. Fractional distillation. ^3He can be viewed either ~~either~~ as a pure substance with a nuclear polarization, P , or as a binary mixture of two chemical species: $^3\text{He}_\uparrow$ and $^3\text{He}_\downarrow$ (differentiated by their nuclear spin) with a concentration x_\uparrow and x_\downarrow . The $^3\text{He}_\uparrow$ and be separated from the $^3\text{He}_\downarrow$ in a fractional distillation column operating with pure ^3He , because the liquid and gas phase will have a different polarization and thus a different chemical composition if the liquid becomes degenerate. This method has never become operational. Castaing and Nozières have pointed out that the same principle also applies to coexisting dilute and concentrated ^3He , where the dilute and the concentrated phase play the role of the gas and the liquid phase.⁴ Nacher *et al.*¹¹ have been the first to show that this method works and they have obtained an enhancement of the polarization in the dilute phase of 3.5 with respect to the equilibrium value of 1.4% at $T \approx 100$ mK.
3. Dilution. This method is based on the same principles as fractional distillation. The difference is that the phase transformations needed for the fractional distillation process are driven by work instead of heat. The latent heat of dilution becomes available to cool the sample, while it is being polarized. This is the method used in the experiments reported in this paper.

We have produced cold polarized liquid ^3He inside the mixing chamber of a ^4He circulating dilution refrigerator (Leiden Dilution Refrigerator, LDR), operating in an external field of 7 T.¹² The minimum temperature in the mixing chamber increases from 8 to 14 mK when the polarization increases from 2 (the equilibrium value) to 15 % because of entropy production due to diffusion and relaxation of the out of equilibrium polarization. The low temperature favors the homogeneity of temperature and magnetization because the temperature dependence of the time constants for thermal and spin equilibrium, $\tau_t \propto T^2$ and $\tau_s \propto T^2$, while $T_1 \propto T^{-2}$ if wall relaxation is suppressed, as we believe nearly to be the case in our experiments. At $p = 6$ bar and $T = 14$ mK, we measure $T_1 \approx 7000$ s and we estimate $\tau_t = l^2/D_t = 2.5$ s and $\tau_s = l^2/D_s = 10$ s, where l is the characteristic radius of our sample ($l = 2$ mm), and D_t and D_s are the thermal¹³ and spin diffusion¹⁴ coefficients. Those conditions compare favorably with the conditions of the rapid melting experiment mentioned above.⁸

For a system with an out of equilibrium polarization, we define an effective magnetic field, B , which is equal to the external field necessary to produce the same polarization in equilibrium. Although P can be measured directly, B can only be obtained through other thermodynamic quantities. Attempts to obtain the magnetic equation of state, $P(B)$, of pure ^3He have ~~made~~ use of the phase equilibrium between solid and liquid ^3He ,¹⁵ between vapor and liquid ^3He ,¹⁶ the velocity of first sound¹⁷ and the heat release due to relaxation of the nuclear polarization.⁷ In this paper we present results on the osmotic pressure of the dilute phase of a saturated ^3He - ^4He mixture as a function of the polarization of the concentrated phase in the mixing chamber of the dilution refrigerator. The osmotic pressure at low polarization ($< 7\%$) agrees well with thermodynamics. The observed polarization dependence of the osmotic pressure in the range 7–15 % is not understood.

made

The layout of the paper is the following. The thermodynamics of saturated polarized ^3He - ^4He mixtures with respect to the solubility and osmotic pressure is discussed in Sec. II. In Sec. III, we review the principles of fractional distillation and discuss its application to the production of polarized ^3He . The similarity between a fractional distillation column and a ^3He - ^4He dilution refrigerator is stressed to show that a process very similar to polarizing ^3He by fractional distillation may take place in a ^4He circulating dilution refrigerator. Section IV describes the design and construction of such a ^4He dilution refrigerator and of the osmotic pressure gauge. In Sec. V we present and discuss the experimental results: (1) The pressure dependence of the polarization enhancement in the LDR allows to determine the pressure where the molar susceptibility of the concentrated

and dilute phase are equal, demonstrating that the susceptibility scale of the data by Ahonen *et al.*¹⁸ is off by 10%. We propose new Fermi liquid parameters for the saturated dilute phase. (2) The evolution of the polarization in the LDR gives T_1 and the circulation rate, two quantities of interest for the analysis of the performance of the LDR as a polarizer. (3) We also present the experimental data on the polarization dependence of the osmotic pressure at $p = 10$ and $p = 16$ bar. Its analysis supports the new Fermi liquid parameters.

II. THE THERMODYNAMICS OF POLARIZED SATURATED ^3He - ^4He MIXTURES

A. The Effective Field

If we consider a polarized ^3He - ^4He mixture as a ternary system, consisting of ^4He , $^3\text{He}_\uparrow$ and $^3\text{He}_\downarrow$ in an external magnetic field B^e , we may write its change of the molar internal energy, du as

$$du = T ds - p dv + \mu_{3\uparrow} dx_\uparrow + \mu_{3\downarrow} dx_\downarrow - \mu_4 dx + B^e dm \quad (1)$$

where s , v , and m are the molar entropy, molar volume and molar magnetic moment of the mixture, T and p are the temperature and the pressure, x_\uparrow , x_\downarrow , $1 - x = 1 - x_\uparrow - x_\downarrow$, $\mu_{3\uparrow}$, $\mu_{3\downarrow}$ and μ_4 are the concentrations and the molar chemical ~~potentials~~ of $^3\text{He}_\uparrow$, $^3\text{He}_\downarrow$ and ^4He . If we only take into account the nuclear paramagnetism of the ^3He , then $m = N_A \gamma (x_\uparrow - x_\downarrow)$ where γ is the nuclear magnetic moment of ^3He and N_A Avogadro's constant. We remark, that the diamagnetic susceptibility is not negligible with respect to the paramagnetic susceptibility, but the diamagnetic susceptibility does not affect the phase equilibrium between the concentrated and dilute phase by cancellation (as can be seen from the derivations in Secs. IIB and IIC).

Eq. (1) can be transformed into

$$du = T ds - p dv + \mu_3 dx - \mu_4 dx + B dm \quad (2)$$

where $\mu_3 = (\mu_{3\uparrow} + \mu_{3\downarrow})/2$ and $B = B^e + (\mu_{3\uparrow} - \mu_{3\downarrow})/2N_A$. The effective field, defined by $B \equiv (\partial u / \partial m)_{s,v,x}$, at any polarization equals the external field, B^e , needed to create the same polarization in equilibrium, i.e. if $\mu_\uparrow = \mu_\downarrow$.

Figure 1 shows the relation between B , B^e , μ_3 , $\mu_{3\uparrow}$ and $\mu_{3\downarrow}$ for polarized ^3He at zero temperature. It also illustrates that μ_3 and B are independent of the polarization being in or out of equilibrium with the external magnetic field. This means, that the equilibrium conditions for a

potentials

μ

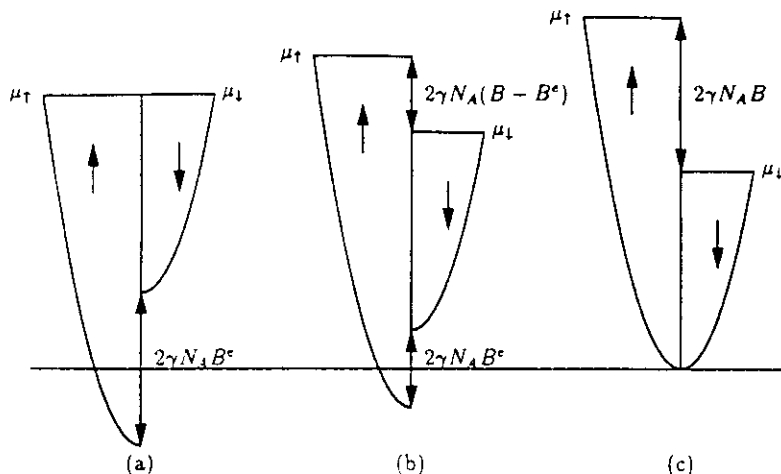


Fig. 1. The Fermi seas for $^3\text{He}_1$ and $^3\text{He}_2$ at $T=0$: (a) $^3\text{He}_1$ polarized by brute force in an external field, B^* , (b) $^3\text{He}_1$ with the same polarization but in a smaller external field and (c) $^3\text{He}_1$ with the same polarization but in zero external field. The effective magnetic field, $B = B^* + (\mu_1 - \mu_2)/2N_A\gamma$ and the chemical potential, $\mu = (\mu_1 + \mu_2)/2$, are equal in all three cases. The phase equilibrium between two polarized Fermi liquids does not depend on the polarization being in or out of equilibrium with the external field.

system of two polarized coexisting phases is independent of the fact that the polarization is produced by brute force or out of equilibrium methods.

B. The Magnetic Field Dependence of the ^4He Chemical Potential and the Osmotic Pressure of a Saturated ^3He - ^4He Mixture

To derive the dependence of the osmotic pressure on B , T and p of a saturated ^3He - ^4He mixture, we start from the Gibbs-Duhem equation for the dilute and concentrated phase

$$\begin{aligned} x_{ds} d\mu_3 + (1 - x_{ds}) d\mu_4 &= -m_d dB - s_d dT + v_d dp \\ x_{cs} d\mu_3 + (1 - x_{cs}) d\mu_4 &= -m_c dB - s_c dT + v_c dp \end{aligned} \quad (3)$$

where T , p , μ_4 as well as μ_1 and μ_2 and hence μ_3 and B are identical in the two phases because of phase equilibrium and x_{cs} (x_{ds}) is the ^3He concentration in the saturated concentrated (dilute) phase. Those equations are valid for systems with an out of equilibrium polarization in zero external field, an equilibrium polarization in an external field, as well as an out of

equilibrium polarization in an external field, provided that B is interpreted as the effective field. Eq. (3) can be simplified by the following approximations:

1. Below 100 mK the concentrated phase is nearly pure: $x_{cs} \approx 1$, $m_c \approx m_{30}$, $s_c \approx s_{30}$, and $v_c \approx v_{30}$, where m_{30} , s_{30} and v_{30} are the molar magnetic moment, molar entropy and molar volume of pure liquid ^3He .
2. The ^4He in the dilute phase does not contribute to the molar magnetic moment and the ~~molar~~ entropy: $m_d = x_{ds} m_{3d}$ and $s_d \approx x_{ds} s_{3d}$, where m_{3d} and s_{3d} are the molar magnetic moment and the molar entropy of the ^3He dissolved in the mixture. s_{4d} can be neglected with respect to s_{3d} below 100 mK.
3. $v_d \approx v_{40}(1 + \alpha x_{ds})$, where v_{40} is the molar volume of pure ^4He and α is nearly independent on concentration and temperature.¹⁹ We assume here that α depends only on the pressure.

molar

After elimination of $d\mu_3$, we obtain:

$$\left(\frac{\partial \mu_4}{\partial B}\right)_{p,T} = -\frac{x_{ds}(m_{3d} - m_{30})}{1 - x_{ds}} \quad (4)$$

$$\left(\frac{\partial \mu_4}{\partial T}\right)_{B,p} = -\frac{x_{ds}(s_{3d} - s_{30})}{1 - x_{ds}} \quad (5)$$

$$\left(\frac{\partial \mu_4}{\partial p}\right)_{B,T} = \frac{(1 + \alpha x_{ds})v_{40} - x_{ds}v_{30}}{1 - x_{ds}} \quad (6)$$

In this paper, we study the ^4He chemical ~~potential~~ through the osmotic pressure, $\Pi(p, T, x, B)$. Π is defined by the relation $\mu_{4d}(p, T, x, B) = \mu_{40}(p - \Pi, T, B = 0)$, where the temperature is assumed to be low enough to neglect the fountain pressure. If we expand this equation to first order and neglect contributions due to the compressibility of ^4He , we obtain $v_{40}\Pi \approx \mu_{40}(p, T, B = 0) - \mu_{4d}(p, T, x, B)$ and find

potential

$$\left(\frac{\partial \Pi}{\partial B}\right)_{p,T} = \frac{x_{ds}(m_{3d} - m_{30})}{v_{40}(1 - x_{ds})} \quad (7)$$

$$\left(\frac{\partial \Pi}{\partial T}\right)_{B,p} = \frac{x_{ds}(s_{3d} - s_{30})}{v_{40}(1 - x_{ds})} \quad (8)$$

$$\left(\frac{\partial \Pi}{\partial p}\right)_{B,T} = -\frac{x_{ds}((1 + \alpha)v_{40} - v_{30})}{v_{40}(1 - x_{ds})} \quad (9)$$

 x_{ds}

Equations (8) and (9) have been derived by Ghazlan and Varoquaux²⁰ but we believe that our derivation is simpler. We emphasize the similarity of Eq. (7) with the Clausius-Clapeyron equation for the magnetic field dependence of the melting curve: $(\partial p/\partial B)_T = (m_s - m_l)/(v_s - v_l)$, where the indices s and l stand for solid and liquid.

C. The Magnetic Field Dependence of the Saturation Concentration of a Dilute ^3He - ^4He Mixture

The concentrations of ^3He in the coexisting dilute and concentrated phase, x_{ds} and x_{cs} , are determined by the condition that the chemical potentials in the two phases are equal:

$$\mu_{3d}(p, T, x_{ds}, B) = \mu_{3c}(p, T, x_{cs}, B) \quad (10)$$

$$\mu_{4d}(p, T, x_{ds}, B) = \mu_{4c}(p, T, x_{cs}, B) \quad (11)$$

Eq. (11) can be immediately eliminated by the approximation $x_{cs} = 1$. We evaluate $\mu_{3d}(B)$ by means of the relation

$$\mu_{3d}(B) = \mu_{3d}(0) + \int_0^B \left(\frac{\partial \mu_{3d}}{\partial B} \right)_{T, p, x_d} dB \quad (12)$$

By inspection of the molar Gibbs free energy of the dilute phase, $g_d = u_d - Ts_d + pv_d - Bm_d = x_d\mu_{3d} + (1 - x_d)\mu_{4d}$, and its differential, $dg_d = -s_d dT + v_d dp + (\mu_{3d} - \mu_{4d}) dx_d - m_d dB$, we obtain

$$\mu_{3d} = g_d + (1 - x_d) \left(\frac{\partial g_d}{\partial x_d} \right)_{T, p, B} \quad (13)$$

Combination of Eqs. (12), (13) and $\partial g_d/\partial B = -m_d = -x_d m_{3d}$ leads to

$$0 = \mu_{3d}(x_{ds}, B) - \mu_{30}(B) = \mu_{3d}(x_{ds}, 0) - \mu_{30}(0) - \int_0^B dB \left(m_{3d} + x_{ds}(1 - x_{ds}) \left(\frac{\partial m_{3d}}{\partial x_d} \right)_{x_{ds}} - m_{30} \right) \quad (14)$$

Expansion of the right hand side of this equation to first order around $x_0 = x_{ds}(B=0)$ and use of $\mu_{3d}(x_0, 0) = \mu_{30}(0)$ gives

$$x_{ds} = x_0 + \frac{1}{(\partial \mu_{3d}/\partial x_d)_{x_0, B=0}} \int_0^B dB \left(m_{3d} + x_0(1 - x_0) \left(\frac{\partial m_{3d}}{\partial x_d} \right)_{x_0} - m_{30} \right) \quad (15)$$

which reduces for low polarization ($m_{3d,0} \approx \chi_{3d,0} B$) to Eq. (15) of Dalfovo and Stringari.²¹

$$x_d = x_0 + \frac{1}{2(\partial\mu_{3d}/\partial x_d)_{x_0, B=0}} \left[\left(1 + (1-x_0) \frac{x_0}{\chi_{3d}} \left(\frac{\partial\chi_{3d}}{\partial x_d} \right)_{x_0} \right) \chi_{3d} - \chi_{30} \right] B^2 \quad (16)$$

D. Discussion

A comment on contradictory predictions in the literature with respect to the polarization or effective field dependence of $x_{c,3}$ is in order.^{4,21-23} Figure 2 shows the magnetic temperature, T_c^* and T_d^* of the concentrated and dilute phase. $T_{c,d}^*$ are defined by the relation $m_{3c,d} = \chi_{3c,d} B = N_A \gamma^2 B / k_B T_{c,d}^*$. At low pressure, $\chi_{3d} > \chi_{3c}$ and at high pressure $\chi_{3d} < \chi_{3c}$. For an ideal Fermi gas $(x_0/\chi)(\partial\chi/\partial x_0) = -2/3$. An analysis of the data of Ref. 18 results in -0.5 ± 0.12 .²⁰ We conclude also using the solubility data of Ref. 19 at $B=0$, that according to Eq. (16) the maximum solubility

of
according

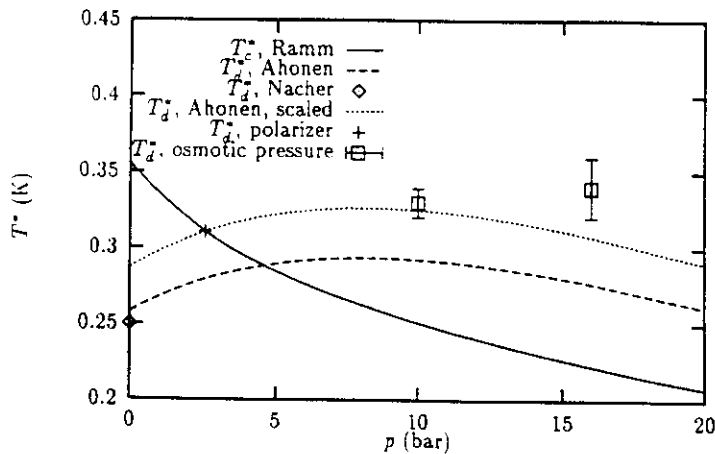


Fig. 2. The magnetic temperatures, T_c^* and T_d^* of the dilute and concentrated phase versus pressure: T_c^* is known with a high absolute accuracy because it is scaled against the paramagnetic susceptibility of solid ^3He .^{30,31} T_d^* is known with a high relative accuracy but the absolute accuracy is only 7% because of scaling against previous data.^{18,32} Also shown is a point at svp, which follows from a direct experimental comparison of T_d^* and T_c^* .³³ We claim that $T_c^* = T_d^*$ at $p = 2.6 \pm 0.04$ bar, based on the pressure dependence of the behavior of our polarizer and we have scaled the susceptibility of Ref. 18 with a factor 0.9. The data points at 10 and 16 bar are determined from the polarization dependence of the osmotic pressure. The discrepancy at $p = 16$ bar between the scaled data of Ref. 18 and the result obtained by the osmotic pressure can be explained by an error in the maximum solubility results of Ref. 19 at $p > 10$ bar and is discussed in Sec. VC.

$T_c^* = T_d^*$
and

decreases with increasing polarization at any pressure. We remark, that the term $(1 - x_0)(x_0/\chi_{3d})(\partial\chi_{3d}/\partial x_d)_{x_0}$ in Eq. (16) is very easy to forget if one treats the dilute phase as an interacting Fermi gas in a mechanical vacuum instead as a mixture of ^3He and ^4He . This term changes the sign of the effective field dependence of the saturation concentration as predicted by the mechanical vacuum model, from positive to negative if $p < 2.6$ bar and amplifies the ~~negative~~ field dependence if $p > 2.6$ bar.

negative

The disagreement of Eq. (16) with the predictions for the polarization dependence of the saturation concentration in Ref. 22 is also due to what we believe to be misconceptions in the treatment of the thermodynamics. We contest the statements in that paper that the maximum solubility depends on the relative quantities of ^3He and ^4He in the system and on the fact that the polarization is obtained by in or out of equilibrium methods. Considering our preceding remarks concerning Fig. 1 and Eq. (3), we maintain: (1) if the dilute and concentrated phase are in equilibrium with each other, the polarization distributes itself over the dilute and concentrated phase to have the same effective field, B , and (2) the concentration in the dilute phase equals the concentration in an external field necessary to obtain the same polarization in the two phases.

Based on the values of the molar susceptibilities, the osmotic pressure of a saturated mixture increases at low pressure and decreases at high pressure with increasing polarization according to Eq. (7). An expression for the magnetic field dependence at low polarization of the osmotic pressure has been derived by Dalfovo and Stringari²¹:

$$\Pi = \Pi_0 - \frac{x\chi_{3d}}{2v_{40}} \left(\frac{x}{\chi_{3d}} \frac{\partial\chi_{3d}}{\partial x} \right) B^2 \quad (17)$$

The osmotic pressure increases with increasing polarization, if x is held constant. We remark that Eqs. (17), (16) and (7) are consistent, because

TABLE I

The Magnetic Field Dependence of the Osmotic Pressure, $\Pi = \Pi_0 + (\partial^2\Pi/2\partial B^2)B^2$, at Constant Concentration, $x = x_0 = x_d$ ($T=0$, $B=0$), and Along the Phase Separation Line, $x = x_d$ ($T=0$, B). For the Calculation, We Have Used the Susceptibility of Ref. 18. Scaled to Agree with the Pressure Dependence of the Polarizer and Shown in Fig. 2

p (bar)	$(\partial^2\Pi/2\partial B^2)_{x_0}$ ($\mu\text{bar T}^{-2}$)	$(\partial^2\Pi/2\partial B^2)_{x_d}$ ($\mu\text{bar T}^{-2}$)
0.0	0.1061	0.04399
10.0	0.1464	-0.09557
20.0	0.1571	-0.1371

Eq. (17) reduces to Eq. (7) after application of the change in concentration given by Eq. (16). The effect of the decrease of x_d due to the polarization is shown in Table I.

We have chosen to measure the polarization dependence of Π instead of x_d because the quantity of polarized dilute phase is very small in our polarizer, which poses technical problems for the measurements of x_d and because of the poor precision of the data for $\partial\mu_d/\partial x_0$ and $(x_0/\chi_{3d})(\partial\chi_{3d}/\partial x_0)$, which renders measurements of x_d more difficult to interpret than those of Π .

III. FRACTIONAL DISTILLATION AND DILUTION

A. Fractional Distillation in a Binary Mixture and its Application to $^3\text{He}_1$ - $^3\text{He}_2$

We review the ~~principle~~ of fractional distillation with the help of Fig. 3. Figure 3a shows an ideal fractional distillation column with a still, two plates and a condenser. The still is heated and the condenser cooled to establish an upward flow of gas from the still through the plates to the condenser and a downward flow of liquid. Figure 3b shows the boiling and dew temperature, T_B and T_D , for an azeotropic binary mixture Y-Z as a function of the concentration of Y, x . We assume that the quantity and the concentration of the liquid and gas phase in the still, the two plates and the condenser, are stationary and that the liquid in the still is in state A (see Fig. 3b). Because the total quantity of mixture Y-Z and the concentration in the still are stationary, the molar flow rate and the concentration of the gas leaving for the first plate equals the molar flow rate and the concentration of the liquid returning from the first plate. The gas leaving the still is in equilibrium with the liquid in the still (state B) and the liquid in the first plate should be in state C. This implies that the concentrations in state B and C are equal and that the transformation of the gas arriving at the first plate into liquid is not an equilibrium process. By the same kind of reasoning the gas going from the first plate to the second plate is in state D and the liquid in the second plate in state E. Finally, the gas condensing on the condenser is in state F and the liquid in the condenser in state G. The concentration of the liquid in the condenser and the still are related to each other by the simple geometrical construction shown in Fig. 3b. For an azeotropic mixture, it is impossible to obtain a mixture with a concentration higher than the azeotropic point when starting from below.

Figure 3c shows the effective field of ~~coexisting~~ ^3He liquid and gas or concentrated and dilute ^3He as a function of polarization. In a fractional

principle

coexisting

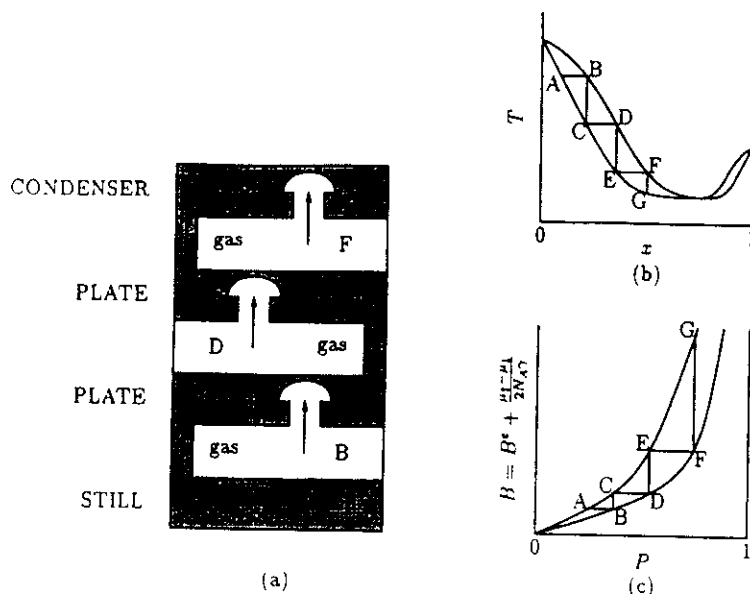


Fig. 3. (a) An ideal distillation setup with a still, a condenser and two plates. (b) The boiling and dew curve of an azeotropic binary mixture Y-Z as a function of the concentration of Y, x . (c) The effective field, B , as a function of polarization, $P = (x_+ - x_-)/(x_+ + x_-)$, for coexisting ^3He liquid and gas or concentrated and dilute ^3He at low pressure. If the distillation process is stationary and the liquid in the still is in state A, then the construction A-B-C-D-E-F-G in Fig. (b) and (c) gives the state of the gas above the still (B), the liquid on the second plate (C), the gas above the first plate (D), the liquid on the first plate (E), the gas above the second plate (F) and the liquid in the condenser (G).

distillation column for the separation of $^3\text{He}_+$ and $^3\text{He}_-$. B and $P = (x_+ - x_-)/(x_+ + x_-)$ play the role of T and x . Again, if the distillation process has reached a stationary state and if $^3\text{He}_+$ and $^3\text{He}_-$ are conserved, we find that the polarization in the still, the two plates and the condenser are related by the same geometrical construction.

The two curves cross each other at ($P=0, B=0$): starting from $P > 0$ one cannot reach a state with $P < 0$ by fractional distillation only. Of course, if at an azeotropic value of the effective field, B_a , the polarization, P_a , of the two phases becomes equal, one is unable to obtain $P > P_a$.

The feasibility of this method has been demonstrated in Ref. 11 in a distillation column working with a saturated ^3He - ^4He mixture. The dilute and concentrated phase may be viewed as the gas and the liquid phase. The dilute phase is created by applying heat ("evaporation") to the concentrated phase in the still and the concentrated phase is created by cooling ("condensation") the dilute phase in the condenser. We emphasize several

distillation

differences between this experiment and the ideal fractional distillation process shown in Fig. 3:

1. $^3\text{He}_c$ —the “liquid” phase—is less dense than $^3\text{He}_d$ —the “gas” phase. To maintain the circulation by heat flow and gravity, the still has to be placed above the condenser.
2. The polarization relaxes due to dipolar interactions in the liquid and interactions with the walls. The relaxation is equivalent to the chemical reaction: $^3\text{He}_l \leftrightarrow ^3\text{He}_g$.
3. To minimize the polarization losses due to the dipolar relaxation, the volume of the liquid to be polarized has to be as small as possible. Therefore, and also for technical simplicity the stack of plates in Fig. 3 has been replaced by a tube. The fractional distillation takes place inside the tube in a counterflow of ascending concentrated droplets in a descending dilute stream.

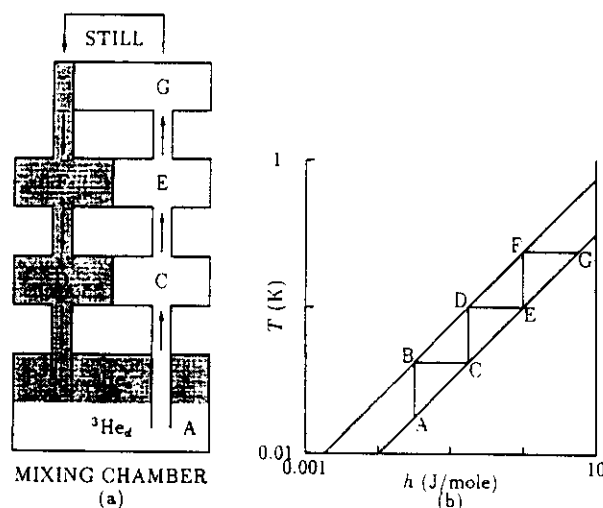


Fig. 4. (a) A dilution refrigerator with a mixing chamber, two step heat exchangers and a still. The arrows indicate direction of the ^3He circulation. (b) The temperature as a function of enthalpy of concentrated and dilute ^3He . If the dilution process is stationary and the dilute phase in the mixing chamber is in state A, then the construction A-B-C-D-E-F-G in Fig. 4b gives the state of the concentrated phase in the mixing chamber (B), the dilute phase in the first heat exchanger (C), the concentrated phase in the first heat exchanger (D), the dilute phase in the second heat exchanger (E), the concentrated phase in the second heat exchanger (F) and the dilute phase in the still (G).

We point out the similarity between a fractional distillation column with plates and a dilution refrigerator with step heat exchangers to prepare the reader for Sec. IIIB. Figure 4 shows the temperature as a function of the molar enthalpy of ^3He in the dilute and concentrated phase, h_{3c} and h_{3d} , and a dilution refrigerator with a mixing chamber, two step heat exchangers and a still. The enthalpy in Fig. 4 plays the role of x in Fig. 3b. In this case, because of enthalpy conservation, the temperature in the still, the two heat exchangers and the mixing chamber are related by the same geometrical construction as in Fig. 3b.

B. Polarizing and Cooling ^3He in a Dilution Refrigerator

In a fractional distillation column the phase transformations— $^3\text{He}_c$ to $^3\text{He}_d$ and $^3\text{He}_d$ to $^3\text{He}_c$ —and the counterflow of $^3\text{He}_c$ and $^3\text{He}_d$ between the condenser and the still are driven a heat current to “evaporate” and to “condense” and by gravity to circulate. This is not essential for the separation of $^3\text{He}_l$ and $^3\text{He}_l$. Instead of creating $^3\text{He}_d$ in the still by “evaporation” and $^3\text{He}_c$ in the condenser by “condensation,” one may as well form the $^3\text{He}_c$ and $^3\text{He}_d$ by extraction and injection of ^4He . So, polarized ^3He can be obtained by applying work instead of heat and this work can be used to turn the fractional distillation column into a refrigerator and to cool the polarized ^3He . The device, in which we realize both processes in parallel is a ^4He circulating dilution refrigerator (or Leiden Dilution Refrigerator, LDR) entirely operating in an external magnetic field. The distinctive advantage of this device with respect to a fractional distillation column is that the polarized sample can be cooled below the temperature of the cold bath needed to operate the LDR. In a fractional distillation column, the polarized sample is always warmer than the cold bath.

A schematic drawing of the LDR is shown in Fig. 5. It consists of a mixing chamber above a demixing chamber, connected to each other by a counterflow capillary. The LDR is filled with a saturated ^3He - ^4He mixture so that the phase separation interface sits in the demixing chamber. The mixing chamber and the exchanger are filled with concentrated ^3He , floating on top of the dilute phase. Superfluid ^4He is extracted through a superleak from the demixing chamber to create concentrated ^3He and heat has to be extracted from the demixing chamber to keep the temperature constant, because of the difference in molar enthalpies ($h_{3d} > h_{3c}$). The ^4He is injected into the mixing chamber to form dilute ^3He and the dilution process cools the mixing chamber. The circulation of superfluid ^4He maintains a counterflow in the capillary of descending dilute ^3He droplets and ascending concentrated ^3He . The counterflow capillary serves as a ~~heat~~ exchanger to achieve the lowest temperature possible: in case of perfect

stream
heat

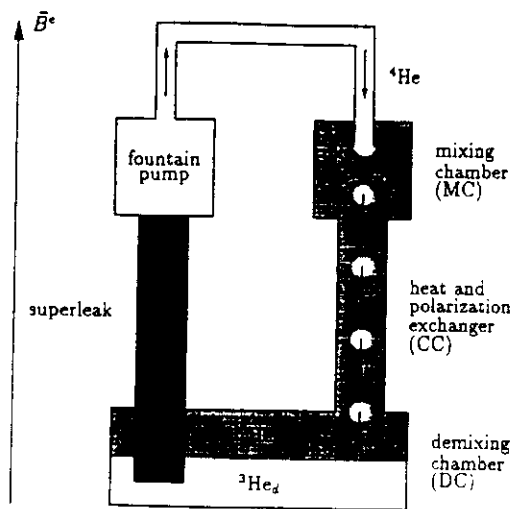


Fig. 5. The ^4He circulating dilution refrigerator in an external magnetic field: superfluid ^4He is extracted from the demixing chamber and injected into the mixing chamber to maintain a counterflow of descending dilute droplets in an ascending stream of concentrated phase in the exchanger. The dilution process cools the liquid in the mixing chamber because of the enthalpy difference between the dilute and concentrated phase. If $P_{3c}(B) > P_{3d}(B)$, it also polarizes ($^3\text{He}_d$ atoms are washed away). Polarizing and cooling are efficient due to the exchange of polarization and heat in the counterflow capillary.

heat exchange, the warm ascending concentrated stream is cooled to the temperature of the mixing chamber by the cold descending dilute droplets before it enters the mixing chamber.

Polarizing by dilution works exactly like cooling by dilution. If the concentrated phase in the mixing chamber has a polarization P_{3c}^m at an effective field B^m , dilute phase with a polarization P_{3d}^m at same effective field B^m will be created by the circulation of ^4He . The $^3\text{He}_d$ falls into the exchanger and will be replaced by a corresponding amount of $^3\text{He}_c$ with a polarization $P_{3c}^m(B^m)$, if the polarization exchange between the dilute and concentrated phase in the counterflow capillary is perfect. At sufficiently high pressure $P_{3c}(B)$ is larger than $P_{3d}(B)$ and the circulation of dilute and concentrated ^3He increases P_{3c}^m . The evolution of P_{3c}^m is ~~governed~~ by the balance between gain due to circulation and losses due to magnetic relaxation in the mixing chamber itself and to spin diffusion towards the demixing chamber which gets depolarized by the circulation for the same reasons as the mixing chamber gets polarized.

and

governed

Visual observation of the flow in LDRs has shown that the best performance is obtained if the dilute phase in the exchanger consists of falling droplets instead of a thick film descending the wall of the exchanger.²⁴ Our apparatus has been designed to favor the formation of dilute droplets. We estimate that 15 droplets/s with a diameter of approximately 0.7 mm are formed for a typical ⁴He flow rate of 100 μ mol/s. To simplify the description of the polarization in the exchanger, we make use of the "droplet flow model" which treats the counterflow in the exchanger as a fine mist of falling dilute droplets with a small volume in an ascending stream of concentrated phase. Van Haeringen *et al.*²⁵ have used the same model to derive a differential equation for the temperature in the exchanger. The implications of the droplet flow model are that (1) the exchange of polarization and heat between the concentrated and dilute phase is perfect, therefore B and T depend only on the height in the exchanger, z , and that (2) spin diffusion, spin relaxation and thermal conduction are ~~governed~~ ^{governed} by the concentrated phase. Under those assumptions, the time evolution of the polarization in the exchanger is given by:

$$\frac{\partial P_{3c}}{\partial t} = D_s \frac{\partial^2 (P_{3c} - P_{3c}^e)}{\partial z^2} - \frac{n_3}{n^x} \frac{\partial (P_{3c} - P_{3d})}{\partial z} - \frac{P_{3c} - P_{3c}^e}{T_1} \quad (18)$$

where D_s and T_1 are the spin diffusion coefficient and the relaxation time of ³He_c and depend both on T and P_{3c} , n^x is the number of moles of ³He_c per length in the exchanger and P_{3c}^e in the first term on the right hand side accounts for an inhomogeneous external field over the length of the exchanger. At low polarization, $P_{3c,d} = \chi_{3c,d} B$ and the second term on the right hand side of Eq. (18) can be replaced by $n_3(1-\beta) \partial P_{3c} / \partial z$, where $\beta = T_c^*/T_d^*$ is the ratio of the molar susceptibilities of the dilute and concentrated phase. This simplification is justified, because in our experiments the polarization remains below 15%, being mainly limited by the T_1 in the mixing chamber. It also means that the consequences of possibly interesting behavior of the difference $P_{3c}(B) - P_{3d}(B)$, for example an azeotropic point, on the behavior of the polarizer are masked by the magnetic relaxation.

Equation (18) allows to get an idea of the profile of B along the exchanger. If we neglect the magnetic relaxation in the exchanger and assume that D_s is constant, then $P_{3c} = C_1 + C_2 \exp kz$ where $k = n_3(1-\beta)/n^x D_s$ and C_1 and C_2 are integration constants, which depend on the amount of ³He and the T_1 in mixing and demixing chamber. For our experimental conditions, k is 1–10 cm⁻¹ and the length of the exchanger 7 cm: the polarization is nearly constant close to the demixing chamber and increases exponentially towards the mixing chamber. Thus, the polarization current leaving the demixing chamber is almost entirely due to

the circulation of dilute and concentrated phase because the gradient of the polarization is almost zero close to the demixing chamber. If the magnetic relaxation in the demixing chamber is fast enough, the polarization current leaving the demixing chamber is given by $n_3(1-\beta)P_{3c}^e$. Without relaxation in the exchanger, the polarization current into the mixing chamber is given by the current leaving the demixing chamber and we obtain

$$\frac{\partial P_{3c}^m}{\partial t} = \frac{n_3}{n^m} (1-\beta) P_{3c}^e - \frac{P_{3c}^m - P_{3c}^e}{T_1} \quad (19)$$

where n^m is the number of moles of $^3\text{He}_c$ in the mixing chamber.

If the dominant relaxation mechanism is due to the dipolar interactions, then $T_1 \propto T^{-2}$ and the highest polarization may be expected at the lowest temperature. However, entropy is produced due to relaxation and diffusion of the out of equilibrium polarization and the minimum temperature increases with increasing polarization. We have extended the model of Ref. 25 for the temperature in a LDR to take into account the dissipation due to the polarization. A set of coupled differential equations for T and P_{3c} is given in the appendix. The numerical solutions of those equations justify the hand waving arguments made above.

IV. EXPERIMENTAL SETUP

A. The Dilution Refrigerator

The polarization losses due to ρ magnetic relaxation should be as low as possible in the mixing chamber as well as in the exchanger close to the mixing chamber in order to obtain the maximum polarization. On the other hand, because the demixing chamber is a polarization source, the magnetic relaxation should be there as fast as possible. The choice of construction materials for the mixing chamber and the exchanger has been restricted to those which have in our experience a low surface relaxation rate. Losses due to bulk (dipolar) relaxation can be minimized by polarizing the smallest volume of ^3He possible.

The mixing chamber is made of Araldite coated with Stycast 1266 and has a height of 4 mm and a diameter of 5 mm. Generally, the ^4He is injected into the mixing chamber of a LDR through a superleak to ensure that it has zero entropy. To eliminate any possible surface relaxation due to an injection superleak, we decided to inject the ^4He through a teflon capillary with a ~~diameter~~ of 0.7 mm and a length of 70 mm. The diameter of the injection capillary is a compromise between being small enough for the ^4He flow to expel concentrated phase and being large enough to minimize

2

diameter

dissipation due to mutual friction between the ^3He and the superfluid ^4He present in the injection capillary. The exchanger is a Teflon capillary ($\varnothing = 1.5 \times 1.8$ mm, height = 70 mm) slid into a CuNi capillary for rigidity.

Two vibrating wire viscometer serving as thermometers are mounted in the mixing chamber, one above and one below the rim of the exchanger (see Fig. 5). The viscometers are made of $62 \mu\text{m}$ \varnothing constantan wire with a density of 6.658 g/cc. This includes the insulation, which is left on the wires to prevent direct contact between the polarized liquid and the constantan. The resonance frequency of the wires is 5–7 kHz and the quality factor, slightly field dependent, is 7000–9000 at 4.2 K in vacuum in the 7 T magnetic field. We do not believe that the relative variation of the field over the vibrating wires of less than 10^{-4} affects the thermometry. At the lowest temperatures the quality factor decreases to almost 20. The polarization dependence of the viscosity of pure liquid ^3He , $\eta \propto T^{-2}$, has been found to be given by $\eta(P_{3c}) = \eta(0)(1 + (2 \pm 1) P_{3c}^2)$.²⁶ We neglect the temperature error of 2% introduced by a polarization of 15%.

A saddle coil is wound on the outside of the mixing chamber to measure the magnetization by continuous wave NMR. From the behavior of the vibrating wires, we know that the mixing chamber is entirely filled with concentrated phase except for the falling dilute droplets. We estimate the volume of the droplets to be less than 1% of the volume of the mixing chamber and we conclude that the NMR signal is practically entirely due to the polarized concentrated phase. The sensitivity of CW NMR spectrometer is calibrated against the known equilibrium polarization of the concentrated phase.

The demixing chamber is made out of copper with silver sinter heat exchangers having an estimated exchange area of 30 m^2 and is cooled by a conventional ^3He circulating dilution refrigerator. The ^4He is circulated by means of fountain pump, sitting on a superleak (15 cm long, 2.5 mm \varnothing) made out of Al_2O_3 powder with a ~~mean~~ particle diameter of $0.15 \mu\text{m}$. The ^4He leaving the fountain pump is thermalized on the still, the heat exchangers and the mixing chamber of the conventional dilution refrigerator before entering the mixing chamber of the LDR.

The whole LDR is placed inside a superconducting magnet. The field at the mixing chamber is 7 T and is about 15% lower at the top of the demixing chamber.

mean

e

B. The Osmotic Pressure Gauge

The osmotic pressure gauge is based on the design of Ref. 27 and is connected to the injection capillary as is shown in Fig. 6. It consists of a stretched $50 \mu\text{m}$ thick Kapton membrane, glued between two charged

Araldite pieces with a spherically concave surface to leave space for the dilute ^3He and pure ^4He . The two sides are connected to each other by a superleak. The ^4He on the pure side of the gauge has a tendency to decrease the concentration of dilute phase on the other side. Therefore, the pressure on the pure side decreases with respect to the dilute side. The pressure drop over the superleak and the membrane equals the osmotic pressure, defined in Sec. IIB. The osmotic pressure gauge resists large differential pressures (1-10 bar) because the concave surfaces have a shape very close to that of the deformed membrane. Gold electrodes have been evaporated on the concave surfaces of the Araldite pieces and on both sides of the Kapton membrane to measure the deflection of the membrane capacitively. We have measured the capacitance only on the pure ^4He side to be independent on changes of the dielectric constant due to a varying ^3He concentration.

After testing the permeability of ^3He for several superleak materials, we have chosen Vycor for the construction of the superleak between the pure and the dilute side of the osmotic pressure gauge. The superleak consists of a Vycor rod with a length of 20 mm and a diameter of 1.5 mm glued into a charged Araldite cylinder. A buffer volume of 5 cm^3 , connected to the pure side of the superleak and thermalized to the mixing chamber of the ^3He circulating dilution refrigerator, decreases the consequences of a

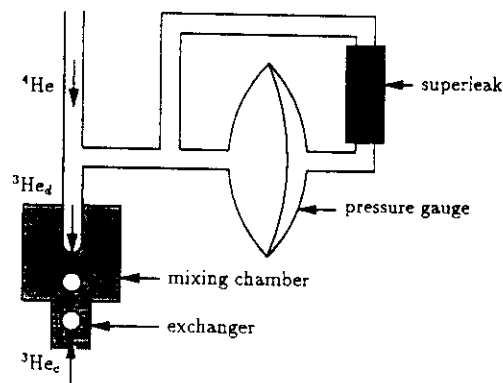


Fig. 6. The osmotic pressure gauge is connected to the injection capillary and is sensible to the osmotic pressure determined by temperature, pressure and effective field of the phase separation interface inside the mixing chamber and chemical potential drop due to mutual friction between the "T" in the injection capillary and the phase separation interface.

to the
V

small ^3He leak through the superleak. With this configuration we have seen no sign at all of ^3He traversing the superleak during the experiments.

If the ^4He inside the injection capillary is at rest, the osmotic pressure gauge measures the osmotic pressure determined by the interface, because $\nabla\mu_4 = 0$ even in the case of temperature and concentration gradients between the phase separation interface and the osmotic pressure gauge. If the ^4He moves, mutual friction between the ^4He and the ^3He present in the injection capillary will cause $\nabla\mu_4 \neq 0$ as we will discuss in Sec. VD. In this respect, the osmotic pressure gauge behaves like a real pressure gauge connected to the pumping line of a pumped bath.

In preliminary experiments, pressure changes in the LDR due to the changing ^4He level in the cryostat have caused osmotic pressure changes, comparable to the changes due to the polarization. In this experiment, we have kept the pressure constant by means of a pressure transducer²⁸ and a control volume with a heater weakly thermalized to the 1 K pot in the fill line of the LDR. The pressure is regulated by changing the temperature of the control ~~volume~~ with a feedback loop using the change in density of ^4He of about 20% between 2 and 4 K. The response time of the feedback loop is less than 1 s and the pressure stability better than 100 μbar . According to Eq. (9) this corresponds to an osmotic pressure stability better than 0.1 μbar , if $p > 5$ bar.

We mention one other source of possible systematic errors: the osmotic pressure gauge is mounted approximately 25 cm above the phase separation interface in the mixing chamber. The hydrostatic pressure difference between the phase separation interface and the osmotic pressure gauge is on the ~~order~~ of 2.5 mbar but its consequences on μ_4 are identical for the dilute phase and pure ^4He side and amount to a decrease in pressure with negligible offset in Π .

The osmotic pressure gauge has been calibrated in an earlier experimental run at 4.2 K against a baratron, changing the pressure by means of ^4He gas. The difference of the dielectric constant between ^4He gas and liquid changes the pressure calibration by 5 mbar. Our value of the osmotic pressure at $p = 10$ bar, $T = 0$ K and $P = 2\%$ is 3% higher than the value given in Ref. 29.

V. RESULTS AND DISCUSSION

In Sec. VA, we describe how the pressure dependence of the polarization enhancement in the polarizer allows to scale the susceptibility of the dilute phase as measured by Ahonen *et al.*¹⁸ and we discuss the implications on the Fermi liquid parameters of saturated $^3\text{He}_d$. In Sec. VB we exploit the dynamic behavior of the polarizer to extract the circulation rate

volume

order

and the magnetic relaxation time, T_1 . In Sec. VC we analyze the polarization and temperature dependence of our osmotic pressure data, postponing the analysis of the effect of mutual friction between ^3He and the superfluid ^4He in the injection capillary on the osmotic pressure to Sec. VD.

A. The Pressure Dependence of the Polarization Enhancement in the Polarizer: The Susceptibility and the Fermi Liquid Parameters of the Dilute Phase

Equation (18) shows that under the condition of perfect exchange the mixing chamber gains polarization with respect to equilibrium due to the counterflow of dilute and concentrated phase if $P_{3c}(B) > P_{3d}(B)$ and it loses polarization if $P_{3c}(B) < P_{3d}(B)$. We have varied the pressure in the dilution ~~refrigerator~~ and observed that below $p = 2.60 \pm 0.04$ bar the stationary polarization in the mixing chamber is lower than the equilibrium value and above $p = 2.60$ bar higher. Therefore, we conclude that $P_{3c}(B) = P_{3d}(B)$ and hence $T_c^* = T_d^*$ at $p = 2.60 \pm 0.04$ bar.

refrigerator

This result might depend on systematic errors due to the temperature and external magnetic field differences between the demixing and the mixing chamber. The temperature difference is not important because the temperature in the demixing chamber remains below 30 mK and temperature corrections to $P_{3c}(B)$ and $P_{3d}(B)$ are negligible. If $P_{3c}(B) = P_{3d}(B)$, then $P_{3c} = P_{3c}^*(z)$ is a solution of Eq. (18) and the magnetic field difference (the external field at the demixing chamber is 15% lower than at the mixing chamber) does not affect the pressure at which we observe that $T_c^* = T_d^*$ in case of perfect exchange. On the other hand, the stationary polarization in the mixing chamber would tend to decrease with respect to its equilibrium value in case of imperfect exchange, because the concentrated phase is coming from the low field region. Therefore, if the exchange is imperfect, the pressure at which we observe $T_c^* = T_d^*$ might be higher but not lower than its real value.

Our result is indicated by a cross in Fig. 2 and has to be compared with the NMR experiments on pure ^3He ^{30,31} and dilute ^3He .¹⁸ The susceptibility of pure ^3He is known with a high absolute accuracy because it has been calibrated against the paramagnetic susceptibility of solid ^3He .³⁰ The susceptibility scale in the work of Ahonen *et al.*¹⁸ has been set by comparison with previous susceptibility measurements.³² Using the quoted error bars,^{32,18} we estimate the uncertainty in the susceptibility scale to be on the order of 7%. We have calculated T_d^* on the phase separation line using the susceptibility data given by Ahonen *et al.* and the molar volume and the saturation concentration given by Ref. 19. Figure 2 shows T_c^* (Ramm) and T_d^* (Ahonen) as a function of pressure. Also shown is T_d^* at

svp (Nacher), calculated from an experimental comparison of the susceptibility of the saturated dilute and concentrated phase.³³ This point agrees well with the susceptibility data by Ahonen *et al.* Also shown are the data by Ahonen *et al.*, but multiplied by an overall scaling factor of 0.9 so that $T_c^* = T_d^*$ at $p = 2.6$ bar (Ahonen scaled), in agreement with the pressure dependence of the polarization enhancement in the polarizer.

Reliable data of the effective mass of the dilute phase, m_d^* , are needed to extract $1 + F_0^a$ from the scaled values of T_d^* . However, the dispersion in m_d^* found in the literature for unsaturated dilute mixtures is large and data for saturated dilute ^3He are hard to find. In our opinion, the best way to get m_d^* on the phase separation line is by means of Eq. (8). We have reanalyzed the temperature dependence of the osmotic pressure data for saturated mixtures of Ref. 29 using x_d and v_{d0} given by Ref. 19 and s_{3c} given by Ref. 34. We find $m_d^* = 2.56, 2.96, 3.28$ at $p = 0.26, 10, 20$ bar respectively. This procedure has the advantage that it relies on thermodynamics only and does not depend on a theoretical model and an effective potential for the ^3He - ^3He interactions in the dilute phase, fitted to the experimental data to calculate m_d^* .³⁵ We think that this procedure is also more reliable than specific heat measurements,^{36,37} because (1) heat flush effects are eliminated and (2) the high temperature corrections to Π are an order of magnitude smaller than those to the specific heat. The value $m_d^* = 2.56$ at $p = 0.26$ bar is in good agreement with the value $m_d^* = 2.55$ at svp, determined from the well known latent heat of dilution and from the temperature dependence of the osmotic pressure dilution.²⁰ We have calculated T_d^* , using the values of m_d^* on the phase separation line and $1 + F_0^a = 0.89$. The standard deviation of those values with respect to the full curve in Fig. 2 is 1%.

We place the concentration dependence of $1 + F_0^a$ at svp in context with the much better established concentration dependence at svp of the spin rotation parameter, $\lambda = 1/(1 + F_0^a) - 1/(1 + F_1^a/3)$. At svp, $\lambda \approx -0.05$ for $x_d < 1\%$, it goes to zero at $x_d \approx 3.5\%$ and continues to increase to nearly 0.04 at the phase separation line.³⁸ At low concentration $1 + F_0^a \approx 1.1$ (see for instance Ref. 39 for a relation between the scattering length, $a = -0.97$ Å, and F_0^a) and on the phase separation line $1 + F_0^a = 0.89$. The concentration dependence of λ can thus be mainly explained by the concentration dependence of $1 + F_0^a$ with a weaker concentration dependence of $1 + F_1^a$.

For the analysis of the polarization dependence of the osmotic pressure in Sec. VC we will need m_d^* at $p = 16$ bar. Therefore, we have inverted the procedure by assuming that $1 + F_0^a = 0.89$ everywhere on the phase separation line to calculate m_d^* . The physical quantities of the dilute phase relevant to the evaluation of the dependence on P_{3c} and T of the osmotic pressure are shown in Table II.

from
other data

$$1 + F_0^a$$

$$1 + F_0^a / 3$$

TABLE II

The Physical Quantities of the Dilute Phase, Relevant to the Evaluation of the Polarization and Temperature Dependence of the Osmotic Pressure, x_{d1} , v_{d0} , and α . Necessary to Calculate the ^3He Density in the Dilute Phase, Are Taken from Ref. 19. See the Text for an Explanation of the Method used to Calculate T_d^* and m_d^*

p (bar)	x_{d1}	v_{d0} (cc/mole)	α	T_d^* (K)	m_d^*	$b = (\partial^2 \Pi / 2 \partial P_{d1}^2)_{T_d^*}$ (mbar)	$c = (\partial^2 \Pi / 2 \partial T^2)_{T_d^*}$ (mbar/K ²)
0	0.0666	27.6	0.285	0.287	2.55	9.176	1088
2	0.0784	27.0	0.263	0.306	2.70	1.744	1199
4	0.0865	26.4	0.245	0.318	2.81	-3.310	1278
6	0.0916	26.0	0.229	0.324	2.90	-6.613	1331
8	0.0943	25.6	0.217	0.326	2.97	-8.699	1365
10	0.0952	25.2	0.206	0.325	3.03	-9.936	1388
12	0.0946	24.8	0.198	0.321	3.08	-10.56	1404
14	0.0931	24.5	0.191	0.315	3.14	-10.74	1417
16	0.0909	24.3	0.185	0.308	3.19	-10.58	1430
18	0.0884	24.0	0.180	0.299	3.25	-10.20	1444
20	0.0859	23.7	0.175	0.290	3.31	-9.731	1461

B. The Circulation Rate and the Relaxation Time

Figure 7 shows the evolution of the polarization, P_{3c} , and the temperature, T , in the mixing chamber to their stationary values at different circulation rates. The circulation rate, \dot{n}_3 , is not known a priori—the values for \dot{n}_3 in Fig. 7 and the rest of the paper follow from the analysis below—and is varied by changing the heating power on the fountain pump, \dot{Q}_{PF} . All data in Fig. 7 have been taken after partial destruction of the stationary out of equilibrium polarization by saturation of the NMR line. This procedure circumvents eventual complications arising from a long magnetic relaxation in the demixing chamber, which may affect the evolution of polarization in the mixing to its stationary value. We believe that during and after saturation, the polarization in the demixing chamber is stationary and remains close to equilibrium while the polarization in the mixing chamber grows. Consequently, Eq. (19) should describe the evolution of the polarization in the mixing chamber reasonably well.

If we define the polarization enhancement in the mixing chamber as $\Gamma \equiv P_{3c}^m / P_{3c}^e$, then Eq. (19) can be rewritten as

$$\frac{d\Gamma}{dt} = 0.85 \frac{\dot{n}_3}{n^m} (1 - \beta) - \frac{\Gamma - 1}{T_1} \quad (20)$$

We remind, that n^m is the amount of concentrated phase in the mixing chamber. The factor 0.85 takes into account the 15% decrease in polarization flow towards the mixing chamber because the equilibrium polarization

time of the

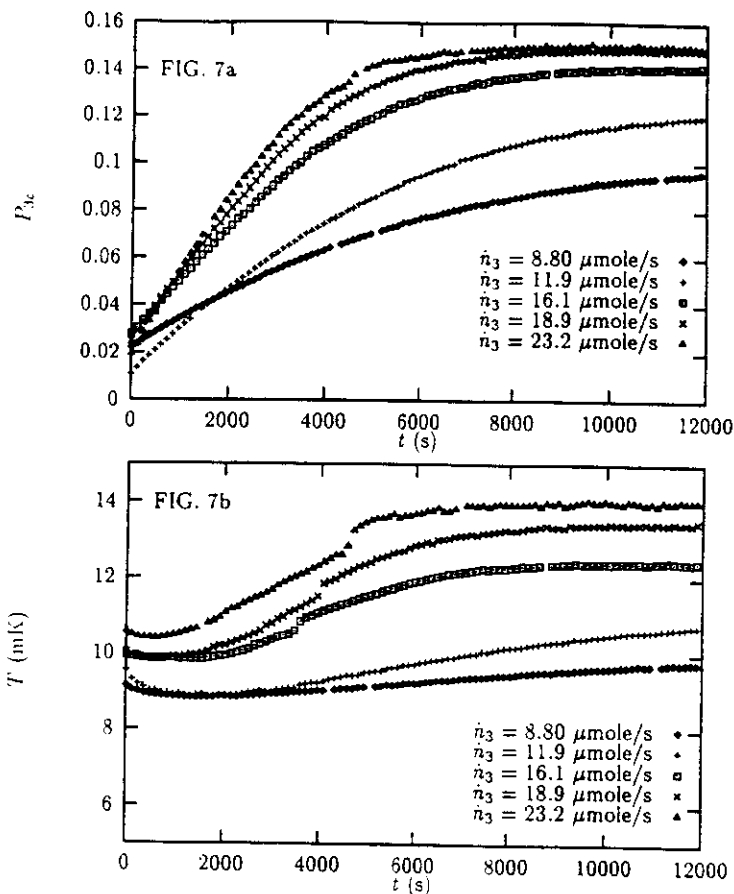


Fig. 7. (a) P_{3c} in the mixing chamber versus time and (b) T in the mixing chamber, both for different values of \dot{n}_3 at $p = 10$ bar after destruction of the polarization by saturation of the NMR line.

in the top of the demixing chamber is 15% lower than in the mixing chamber. We note that we should expect a straight line on plotting $d\Gamma/dt$ versus $\Gamma - 1$, if the ~~relaxation~~ is exponential, i.e. T_1 is constant.

Figure 8 shows $d\Gamma/dt$, obtained by numerical derivation of the data shown in Fig. 7, and T versus $\Gamma - 1$ because T_1 may depend on temperature. We remark, that the scatter in $d\Gamma/dt$ at $\dot{n}_3 = 23.2 \mu\text{mole/s}$ and $5 < \Gamma - 1 < 6$ is due to the sensitivity of the algorithm for calculating $d\Gamma/dt$ to the irregularities in the data at $t \approx 5000$ s in Fig. 7. Figure 8 shows clearly, that the relaxation is non-exponential.

for
r

relaxation

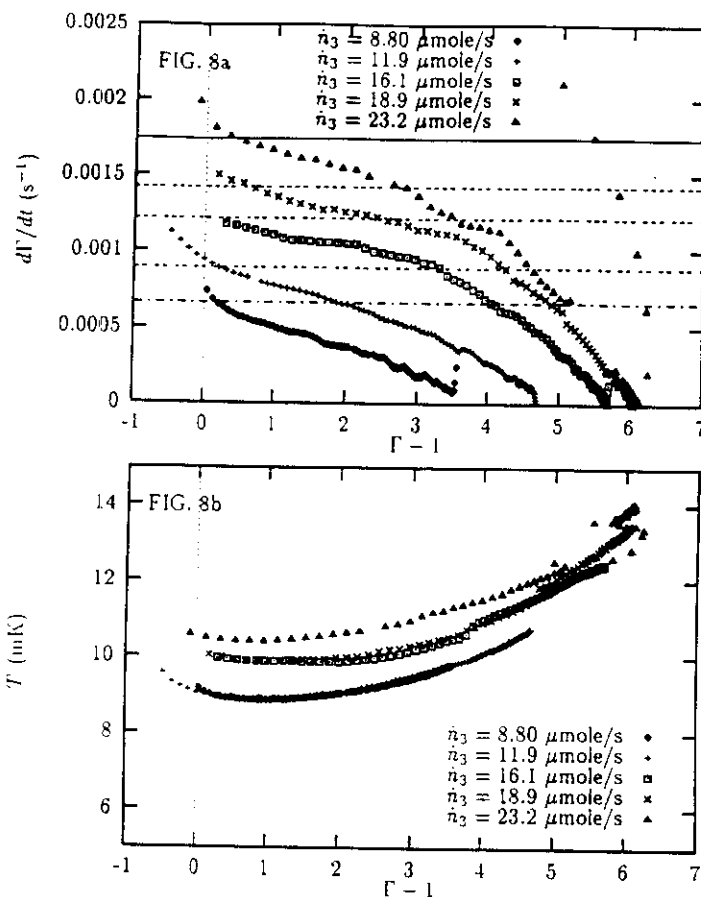


Fig. 8. For different circulation rates at $p = 10$ bar: (a) $d\Gamma/dt$ versus $\Gamma - 1$ and (b) T versus $\Gamma - 1$, where the polarization gain, Γ , is defined as $\Gamma = P_{3c}/P_{3e}^*$. The horizontal lines in Fig. 8a indicate the extrapolated values for $d\Gamma/dt = 0.85\dot{n}_3(1 - \beta)/n^m$ at $\Gamma - 1 = 0$ (the factor 0.85 accounts for the 15% inhomogeneity of the external field over the length of the exchanger).

We have ~~tried~~ to fit Eq. (20) to the points shown in Fig. 8 assuming that T_1 is intrinsic, but allowing for a polarization dependence of T_1 due to the extra phase space available for scattering ($\mu_1 > \mu_1$). In this case, T_1 is given by^{4,40}

tried

$$\frac{1}{T_1} = C_D \left[T^2 + C_I \left(\frac{T^*}{\pi} \right)^2 (P - P^e)^2 \right] \quad (21)$$

where C_D depends on the dipolar interactions and the Fermi liquid parameters but only weakly on polarization, C_I takes into account corrections if the Fermi liquid is strongly interacting ($C_I=1$ for very dilute $^3\text{He}^{40}$) and T_1 is defined by $dP/dt = -(P - P^*)/T_1$. In our experimental conditions $T^*(P - P^*)/\pi$ is nearly as large as T . Equations (20) and (21) do not fit the data with one set (C_D, C_I) for all \dot{n}_3 , indicating the presence of a non-intrinsic relaxation mechanism.

We have extrapolated $d\Gamma/dt$ to $\Gamma - 1 = 0$ to obtain \dot{n}_3 as a function of the power on the fountain pump, \dot{Q}_{PF} . Note, that at $\Gamma - 1 = 0$, $d\Gamma/dt = 0.85\dot{n}_3(1 - \beta)/n^m$. The values for $d\Gamma/dt$ at $\Gamma - 1 = 0$ are 0.00066, 0.00089, 0.00121, 0.00142 and 0.00174 s^{-1} and are indicated by the horizontal lines in Fig. 8a. The flow rate, \dot{n}_3 , calculated for a mixing chamber volume of 80 mm^3 , is shown in Fig. 9 as a function of \dot{Q}_{PF} .

The scatter in the values for \dot{n}_3 is determined by the extrapolation of $d\Gamma/dt$ to $\Gamma - 1 = 0$ and is on the order of 5% as can be seen from Fig. 8. The precision of \dot{n}_3 is also affected by (1) the precision of the correction factor 0.85, (2) the precision of β , (3) the efficiency of the relaxation in the demixing chamber to compensate for the polarization losses, (4) the precision of the volume of the mixing chamber, difficult to estimate because of the glue that has entered during the construction and (5) the relaxation in the capillary close to the mixing chamber which has been neglected. The precision in \dot{n}_3 is estimated to be 10%. We point out that in Ref. 41 the correction factor 0.85 has not been applied.

order

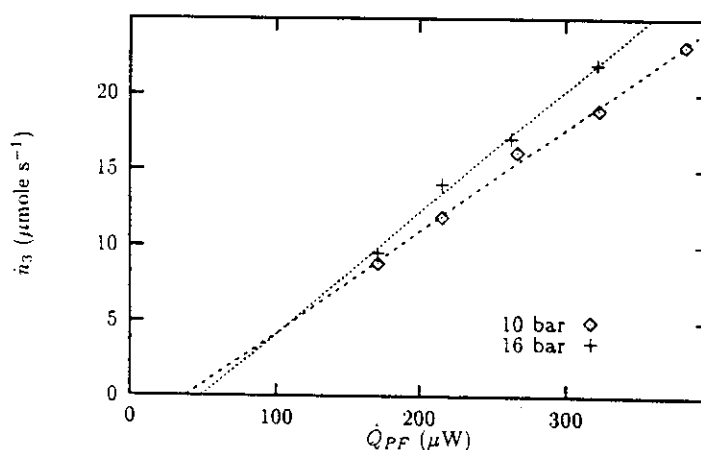


Fig. 9. \dot{n}_3 versus \dot{Q}_{PF} for $p = 10$ and $p = 16$ bar.

In the ideal case, the circulation rate can be obtained from the enthalpy balance on the fountain pump, $\dot{Q}_{PF} = \dot{n}_4 s_4(T_{PF}) T_{PF}$, where $\dot{n}_4 = (1 - x_3)\dot{n}_3/x_3$ is the ⁴He circulation rate, s_4 the molar entropy of ⁴He and T_{PF} the temperature of the fountain pump. If T_{PF} is independent of \dot{Q}_{PF} , which is approximately true in our case, then we expect straight lines going through the origin. However, the data extrapolates back to $\dot{Q}_{PF} \approx 50 \mu\text{W}$ at $\dot{n}_3 = 0$, indicating that a constant part of the heat applied to the fountain pump ($T_{PF} \approx 1.4 \text{ K}$) goes by conduction to the thermalization on the still. Also the slope is much smaller than expected from the enthalpy balance, probably due to dissipation in the capillaries between the fountain pump and the mixing chamber.

In a similar way as for \dot{n}_3 , we have obtained T_1 by application of Eq. (19) using dT/dt at $\Gamma - 1 = 0$ (to determine the polarization gain when the losses due to relaxation are zero) and $\Gamma - 1$ at $dT/dt = 0$ (to determine T_1 , when the gain equals the losses). Figure 10 shows $1/T_1$ as a function of T^2 . Also shown is the theoretical temperature dependence of $1/T_1$ at $p = 0$ and $p = 27 \text{ bar}$ calculated for intrinsic dipolar relaxation.^{42,43} These calculations are in good agreement with experimental data of T_1 at higher temperatures.^{7,42,43} Our data for $1/T_1$ are a factor of 5 bigger than expected from the theory and deviate from the expected temperature dependence. We expect that correcting our data for the polarization dependence

sp

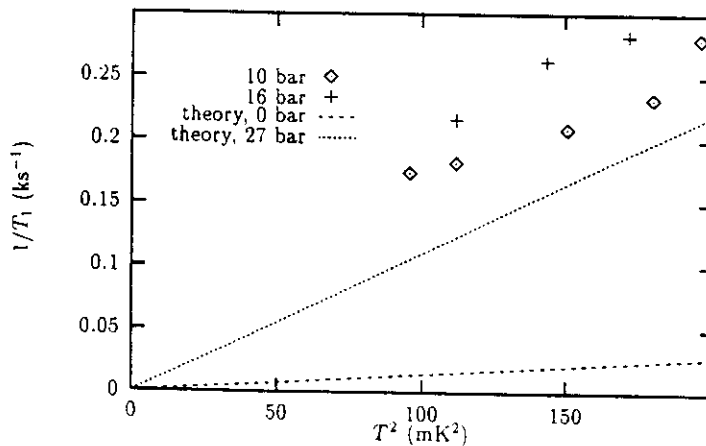


Fig. 10. $1/T_1$, obtained from the polarization current leaving the demixing chamber and the stationary polarization in the mixing chamber, versus T^2 for $p = 10$ and $p = 16 \text{ bar}$. Also shown are the theoretical curves for $1/T_1$ calculated for intrinsic dipolar relaxation at $p = 0$ and $p = 27 \text{ bar}$.^{42,43} We attribute the discrepancy between our data and the theoretical curves to an additional relaxation mechanism, probably due to the surface.

decreases $1/T_1$ by at most 30 %, if T_1 is entirely due to dipolar interactions. Linear extrapolation of our data to $T^2=0$ does not cross the origin, indicating that in addition to the intrinsic dipolar relaxation mechanism there is another mechanism that we attribute to surface relaxation. This also explains why fitting the data in Fig. 8 with Eqs. (19) and (21) fails. We point out that suppression of this surface relaxation mechanism will allow measurements of the polarization dependence of T_1 . The impact of T_1 on the maximum polarization and minimum temperature that can be obtained in the polarizer will be discussed in Sec. VI.

C. The Osmotic Pressure

We resume the different parameters on which the osmotic pressure depends before presenting the experimental results. For sufficiently low T and P_{3c} , the osmotic pressure measured by the gauge is given by

$$\Pi = \Pi_p(p) + b(p) P_{3c}^2 + c(p) T^2 + \Pi_{mf}(\dot{n}_3, p) \quad (22)$$

where the first three terms on the right hand side describe the osmotic pressure at the phase separation interface in the mixing chamber. They follow from integration of Eqs. (9), (7) and (8). Use of $s_{3c,d} = \gamma_{3c,d} T$ leads to $c(p) = x_{ds}(\gamma_{3d} - \gamma_{3c})/2v_{40}(1 - x_{ds})$ and use of $B = k_B T_c^* P_{3c}/\gamma$ and $\chi_{3c,d} = N_A \gamma^2/k_B T_{c,d}^*$ to $b(p) = x_{ds} R T_c^* (T_c^*/T_d^* - 1)/2v_{40}(1 - x_{ds})$. The last term on the right hand side arises from mutual friction between the ^3He in the injection capillary and the superfluid ^4He (see Fig. 6 and Sec. IVB). A detailed discussion of this effect is ~~postponed~~ to Sec. VD, where it has been fully accounted for. We note that Π increases with increasing T and decreases with increasing P_{3c} and \dot{n}_3 .

Figure 11a shows that Π decreases approximately quadratically with increasing P_{3c} . T increases with increasing \dot{n}_3 as is shown in Fig. 11b because of dissipation due to mutual friction. The effect of the mutual friction on Π is the following: on the one hand, it raises Π indirectly through the temperature increase and on the other hand it lowers Π because of the chemical potential drop along the injection capillary. Figure 11a shows, that the direct effect of the mutual friction on Π is larger than the indirect one. Finally, Fig. 11c shows Π as a function of P_{3c}^2 after subtraction of the term $c(p) T^2$ (using $c(p)$ from Table II). The decrease of Π , faster than quadratic in P_{3c} , might be due to systematic errors or an unexpected behavior of $P_{3d}(B)$. We will come back to this issue at the end of this section.

To circumvent the possible systematic errors, we have restricted fitting of the experimental data by Eq. (22) to $P_{3c} < 7\%$. All data have been fitted

postponed

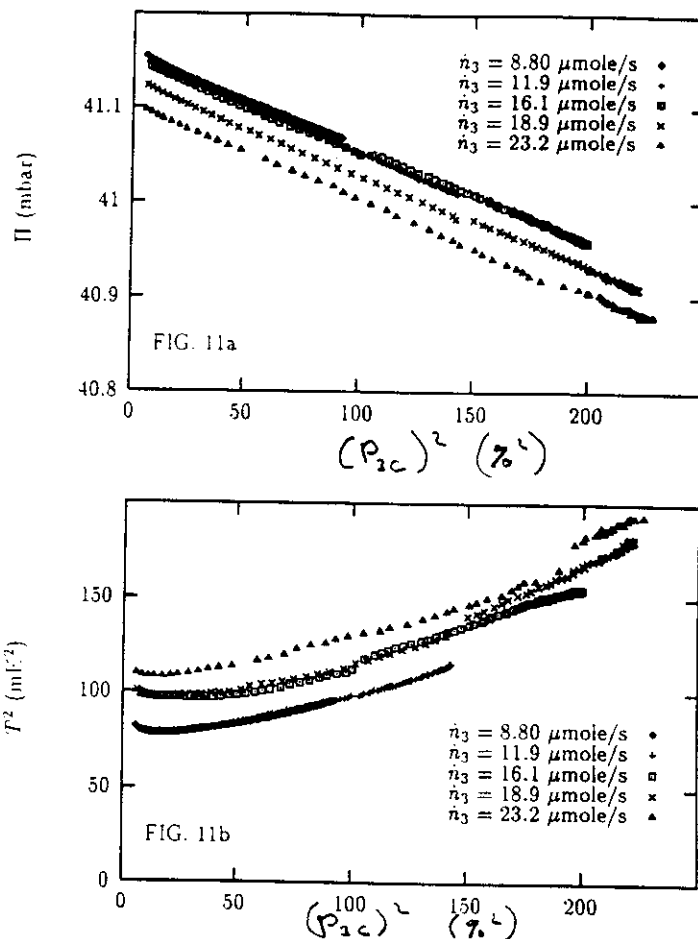


Fig. 11. (a) $\Pi(T, P_{3c})$ versus P_{3c}^2 , (b) T^2 versus P_{3c}^2 and (c) $\Pi(T=0, P_{3c})$ versus P_{3c}^2 for different circulation rates at $p=10$ bar. To illustrate the deviations from the low polarization behavior of the osmotic pressure on P_{3c} , we have added $\Pi = 40.95 - 10.46(P_{3c})^2$ in Fig. 11c.

with one set of parameters $\Pi(p, \dot{n}_3)$, $b(p)$ and $c(p)$. In occurrence, we have used 7 free parameters for 5 different circulation rates at $p=10$ bar and 6 free parameters for 4 different circulation rates at $p=16$ bar. The results for $b(p)$ and $c(p)$ are shown in Table III. We remark that the values of $\Pi(p, \dot{n}_3)$ will be used in Sec. VD. The standard deviation, $\Delta\Pi$, between the experimental data and Eq. (22) is $\Delta\Pi = 2.6 \mu\text{bar}$ for $p=16$ bar and $\Delta\Pi = 1.2 \mu\text{bar}$ for $p=10$ bar.

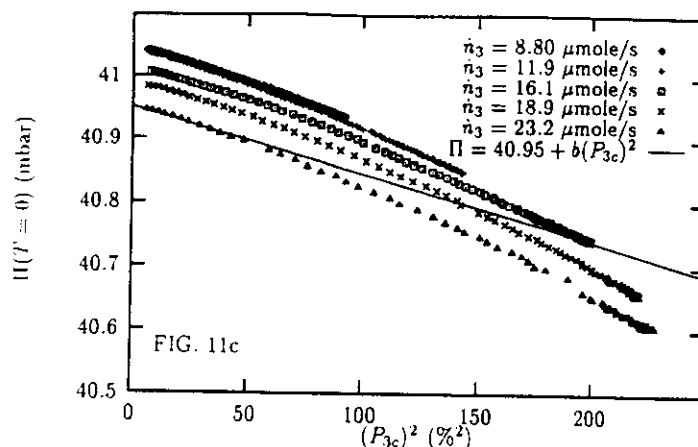


Fig. 11. Continued

The results for $b(p)$ obtained from the osmotic pressure measurements (Table III) are in agreement with the values for $b(p)$ obtained from the Fermi liquid parameters for the dilute phase proposed in Sec. VA (Table II). The results for $c(p)$ do not agree at all. However, fitting Eq. (22) to the experimental data with the values of $c(p)$ from Table II as input does not alter the results for $b(p)$ significantly. T_d^* has been calculated using the values in Table III and the results are shown in Fig. 2. The experimental point for T_d^* at $p = 10$ bar agrees with the scaled data of Ref. 18 within the experimental error bar. The point at $p = 16$ bar does not agree within the error bar, but this can be explained by an error in the data for x_{ds} as given in Ref. 19. Indeed, Fig. 8 of the review paper by Edwards and Pettersen⁴⁴ shows a comparison of these data with those from Ref. 29. All data agree very well below $p = 10$ bar, but at $p > 10$ bar a slight discrepancy sets in and at $p = 16$ bar x_{ds} from Ref. 19 is 2.5% less than an

TABLE III

The Experimental Values for $b = (\partial^2 \Pi / \partial P_{3c}^2)_{T_d}$ and $c = (\partial^2 \Pi / \partial T^2)_{x_{ds}}$ Deduced from the Osmotic Pressure Measurements

p (bar)	b (mbar)	c (mbar K ⁻²)
10	-10.46 ± 0.90	250 ± 210
16	-13.2 ± 1.3	670 ± 510

interpolation of the data of Ref. 29 (i.e. an absolute error of 0.0022). If x_{ds} at $p = 16$ bar is indeed 2.5 % larger than given in Watson *et al.*, the consequences are twofold: (1) the scaled data of Ref. 18 increase by 7.5 mK at $p = 16$ bar and (2) the result of T_d^* at $p = 16$ bar, obtained from the osmotic pressure measurements decreases by 5 mK. In this case, the scaled data of Ref. 18 and the osmotic pressure point for T_d^* agree within the error bar.

Before discussing the physical implications of the faster than quadratic decrease of Π with P_{3c} , we point out two possible systematic errors, which might explain this behavior:

1. A nonlinear sensitivity of the NMR-spectrometer. Two factors may contribute to the nonlinearity in our setup. Firstly, for the impedance of the resonant circuit to vary linearly with the polarization, the effect of the sample on the self inductance of the resonant circuit (depending on the polarization, filling factor and the quality factor) should be small. This condition is approximately met for our polarization but will be violated ~~at~~ *for* higher polarization. Secondly, we measure the impedance of the resonant circuit by comparison with $50\ \Omega$ in a bridge made of a magic T. Instead of measuring the impedance Z of the resonant circuit, this setup measures the absolute value of the ~~reflection~~ *reflection* coefficient, $\Gamma = (Z - Z_0)/(Z + Z_0)$ where $Z_0 = 50\ \Omega$ is the characteristic impedance of the circuit. The variation in Z is sufficiently large for $|\Gamma|$ to depend in a nonlinear fashion on polarization. Several experiments with differently tuned resonant circuits give us confidence that this nonlinearity is not very large. However, we cannot exclude that the maximum polarization is 18 % (the value needed to obtain a quadratic decrease in Fig. 11c) instead of 15 %.
2. A polarization dependent temperature difference between the phase separation interface and the lower viscometer serving as a thermometer. To account for the deviation from a quadratic polarization dependence, the temperature of the interface should be about 5 mK lower than that measured by the viscometer at the maximum polarization. Numerical solution of the Eqs. (A1) and (A4) imposing the boundary condition that the polarization and temperature in the mixing chamber are homogeneous, shows that almost all the polarization gain occurs in the last 0.5 cm of exchanger before the concentrated phase enters the mixing chamber. The most important source of irreversible heating is due to spin diffusion, creating a temperature gradient of about 5 mK/cm over the same 0.5 cm of the exchanger. Although gradients in the

mixing chamber might arise from exchange of heat and polarization already occurring in the mixing chamber, we find it hard to believe that temperature differences of 5 mK exist in the mixing chamber. In previous experiments we have observed that the upper viscometer (closer to the phase separation interface) always indicated a temperature 1.5 mK lower than the lower viscometer, independent of polarization.

We now turn our attention to the consequences of a polarization dependent susceptibility of the concentrated phase assuming that the susceptibility of the dilute phase remains constant. We model $\chi_{3c}(P_{3c})$ by $\chi_{3c}(P_{3c}=0)(1 + \delta P_{3c}^2)$, where $\delta < 0$ for nearly ferromagnetic and $\delta > 0$ for meta-magnetic behavior. Integrating Eq. (7) with χ_{3d} constant, we find that in both cases the decrease of Π with increasing P_{3c} is slower than quadratic if $|\delta|$ is sufficiently large, because the integration limit on the field is set by the polarization of the concentrated phase. Only a measurement of P_{3d} will resolve the ambiguity between nearly ferromagnetic and meta-magnetic behavior. Although Π decreases slightly faster than quadratic in P_{3c} for small negative δ , we never calculate a decrease of Π that much faster than quadratic as shown in Fig. 11c. This implies, that if the behavior of Π in Fig. 11c is true, it can only be explained by a decreasing susceptibility of the dilute phase with increasing B .

D. Mutual Friction Between ^3He and Superfluid ^4He

An extensive study of the dissipation in the dilute phase due to flow in a ^3He circulating dilution refrigerator has been published in Refs. 45 and 46. In these experiments the ^3He has a velocity, v_n , with respect to the superfluid ^4He and the walls of the walls of the exit tube of a mixing chamber. The flow gives rise to a pressure gradient due to viscosity at low v_n and a gradient in the ^4He chemical potential, $\nabla\mu_4$, at high v_n due to mutual friction between the ^3He and the superfluid ^4He . $\nabla\mu_4$ is given by

$$\nabla\mu_4 = f_{mf} \left(\frac{\dot{n}_3}{\sigma} \right)^3 \quad (23)$$

where σ is the cross-section of the tube and f_{mf} has been determined experimentally at svp: $f_{mf} = 1.2 \times 10^{-8} \text{ kg s m}^7 \text{ mol}^{-4}$. The authors of Ref. 46 suggest that a nonzero relative velocity between ^3He and ^4He maintains a vortex tangle in the superfluid which leads to this mutual friction force.

The consequences of the dissipation due to mutual friction in the mixing chamber of a ^4He circulating dilution refrigerator have been discussed by

Geurst *et al.*⁴⁷ However, they could not quantify the dissipation because of lack of experimental data on the mutual friction at the time. To our knowledge, the mutual friction has never been observed in a LDR.

In our LDR, mutual friction occurs between the ^3He and the superfluid ^4He in the injection capillary (^3He dissolves into the superfluid ^4He inside the injection capillary because of the condition $\nabla\mu_4=0$ in the absence of mutual friction). The ^3He atoms form a sort of soft superleak stuck to the wall by viscosity through which the ^4He flows at a speed, v_s . If the mutual friction between the ^3He and ^4He is indeed due to a vortex tangle, $\nabla\mu_4$ is also given by Eq. (23). This effect manifests itself in our experimental setup as a flow rate dependent osmotic pressure change, $\Delta\Pi_{mf}(\dot{n}_3)$, and a flow rate dependent heat leak, $\dot{Q}_{mf}(\dot{n}_3)$. $\dot{Q}_{mf}(\dot{n}_3)$ is dissipated inside the injection capillary, but is transported towards the mixing chamber. We find

$$\Delta\Pi_{mf}(\dot{n}_3) = -\Delta\mu_4/v_{40} = -\frac{f_{mf}L}{v_{40}}\left(\frac{\dot{n}_3}{\sigma}\right)^3 \quad (24)$$

and

$$\dot{Q}_{mf}(\dot{n}_3) = \dot{n}_4 \Delta\mu_4 = \frac{(1-x)\dot{n}_3 f_{mf} L}{x} \left(\frac{\dot{n}_3}{\sigma}\right)^3 \quad (25)$$

where L is the length of the injection capillary.

The minimum temperature of most LDRs starts to fall rapidly with increasing flow rate but becomes constant at higher flow rates. Since the cooling power of the dilution process is given by $\dot{Q}_{dil} = \dot{n}_3(\gamma_{3d} - \gamma_{3c}) T^2$, all those dilution refrigerators are subject to a heat leak which increases linearly with flow rate. Inspection of Eq. (25) shows that such a heat leak originates in the gravitational energy dissipated by the falling droplets. If we assume that our LDR is subject to a heat leak of the form $\dot{n}_3(\gamma_{3d} - \gamma_{3c}) T_g^2$, where T_g is the minimum temperature due to gravitation, and a heat leak of the form $\dot{Q}_{mf}(\dot{n}_3)$, the temperature in the mixing chamber is given (in the absence of dissipation related to the polarization) by

$$T_{min}^2 = T_g^2 + \frac{(1-x)f_{mf}L}{x(\gamma_{3d} - \gamma_{3c})} \left(\frac{\dot{n}_3}{\sigma}\right)^3 \quad (26)$$

Figure 12 shows T_{min}^2 and $\Pi(B=0, T=0) = \Pi_0 + \Delta\Pi_{mf}(\dot{n}_3)$ as a function of $(\dot{n}_3)^3$. T_{min} is the minimum temperature of the mixing chamber, measured after saturation of the NMR line when the polarization and the

(A4)

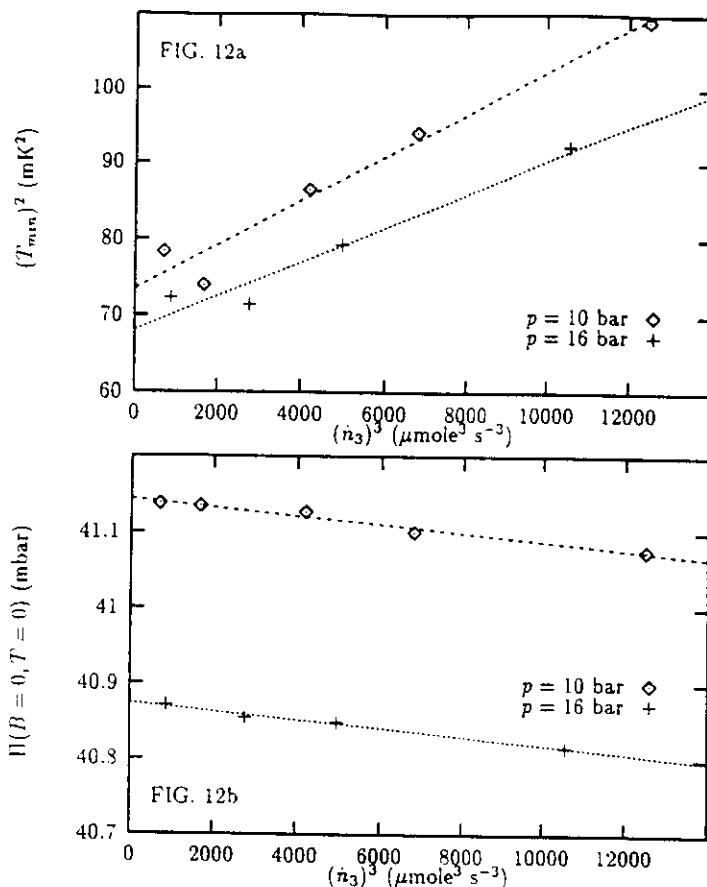


Fig. 12. (a) $(T_{min})^2$ versus $(\dot{n}_3)^3$ and (b) $\Pi(T=0, B=0)$ versus $(\dot{n}_3)^3$ at a pressure of 10 and 16 bar. Also shown are best fits of Eq. (24) and (26) to the data. The agreement between f_{mf} determined from osmotic pressure measurements and from the mixing chamber temperature is reasonable (see Table IV).

losses due to the out of equilibrium are still low. The mutual friction coefficient, f_{mf} , has been obtained by fitting Eqs. (24) and (26) to the experimental data in Fig. 12 and using $L = 70$ mm and $\sigma = 0.385$ mm². The standard deviation of the slope of the fit of Eq. (24) as well as Eq. (26) is 10% introducing an error of 10% in the factor $f_{mf}(\dot{n}_3/\sigma)^3$. The relative accuracy of f_{mf} is on the order of 30%, because of the 10% error in the scale of \dot{n}_3 . The results are shown in Table IV. The agreement between the mutual friction coefficient, f_{mf} , deduced from the osmotic pressure and

TABLE IV

The Mutual Friction Coefficient Between ^3He and Superfluid ^4He Deduced from the Flow Rate Dependence of the Minimum Temperature of the Mixing Chamber, $f_{mf}(T_{mc})$, and the Osmotic Pressure, $f_{mf}(\Pi)$. The scatter in f_{mf} is 10%, Based on the Standard Deviation of the Slope of the Fit of Eqs. (24) and (26) to the Data in Fig. 12. The Relative Error Is on the Order of 30%, Determined by the Error in the Scale of \dot{n}_3 .

p (bar)	$f_{mf}(T_{mc})$ ($10^{-8} \text{ kg s m}^{-2} \text{ mol}^{-4}$)	$f_{mf}(\Pi)$ ($10^{-8} \text{ kg s m}^{-2} \text{ mol}^{-4}$)
10.0	1.65	1.13
16.0	1.26	1.09

deduced from the minimum temperature as a function of circulation rate is reasonable, considering the sensitivity of T_{min} to memory effects of the amount of RF power used for saturation. We conclude, that we have a satisfactory explanation for the dependence of $\Pi(p)$ on circulation rate, justifying the analysis of the osmotic pressure data with Eq. (22) in Sec. VC.

In practice, the heating due to the irreversible processes related to the out of equilibrium polarization is much more important than the heating due to mutual friction. We expect that the performance of the LDR as a polarizer will improve slightly if the mutual friction is eliminated by injection of the ^4He into the mixing chamber through an injection superleak. We have already experimental evidence that an injection superleak does not contribute significantly to the relaxation rate but we have not yet solved all technical problems imposed by the second superleak (the superleaks block, possibly because ^3He migration through the superleaks).

VI. CONCLUSIONS

Dilution of ^3He in ^4He is a suitable nuclear orientation technique to produce very degenerate liquid ^3He with an out of equilibrium but stationary polarization. We have measured the polarization dependence of the osmotic pressure. At low polarization, this dependence is consistent with thermodynamics. At high polarization, it is not clear if the measured polarization dependence of the osmotic pressure is due to experimental errors or to an unexpected dependence of $P_{3d}(B)$.

A criticism of the experiment as presented in this paper is that the analysis in terms of Eq. (7) depends on assumptions made with respect to

the value of $P_{3d}(B)$. Therefore, the effective field B is not really measured. Measurement of Π , P_{3c} and P_{3d} allows the determination of B using Eq. (7) and hence the equations of state $P_{3c}(B)$ and $P_{3d}(B)$.

The interest of polarizing by dilution depends on the minimum temperature and maximum polarization that can be reached. In principle, the experimental conditions in our setup are sufficient to observe nonlinear spin dynamics originating in the Landau field and the dipolar interactions.⁴⁸ A higher external field should increase the polarization and the temperature. The possibility of obtain lower temperatures and higher polarizations depends on the relaxation rate in the mixing chamber: all contributions due to surface relaxation mechanisms should be suppressed. In the limit of dipolar relaxation, the polarization losses due to relaxation and the heat release due to relaxation and spin diffusion are proportional to T^2 . The main contribution to the heating is due to spin diffusion ($\propto (n_3)^2$), which depends also on T_1 through the circulation rate. There is still room for improvement of T_1 in the present experimental setup and higher polarizations at lower temperatures should be possible.

ACKNOWLEDGMENTS

One of us (A. R.) thanks the CNPq (funded by the Brazilian Ministry of Science and Technology) for financing his stay in France. We acknowledge the stimulating discussions with D. M. Lee and M. Tagirov during the preliminary stages of this experiment. The progress of the osmotic pressure measurements has been considerably accelerated by the gift of Vycor glass from the low temperature group at Cornell University. The interest shown in this work by O. Buu, P. Nozières, L. Puech, E. Varoquaux, S. A. J. Wieggers and P. E. Wolf has helped us in the understanding of our experiment. Finally, we thank A. Benoit for his suggestion that an injection superleak in a LDR is not an absolute necessity.

APPENDIX: THE COUPLED EQUATIONS FOR THE POLARIZATION AND THE TEMPERATURE IN THE COUNTERFLOW CAPILLARY

The equations for the polarization and temperature in the exchanger should be helpful in designing a polarizer. They have been derived applying the droplet flow model²⁵: the counterflow is a fine mist of falling dilute droplets in a concentrated stream ascending in the z -direction and the speed of the dilute droplets is much greater than the speed of the rising concentrated phase. Note, that the molar flow rates of concentrated and

dilute ^3He are equal but the amount of dilute ^3He in the exchanger is small with respect to the amount of concentrated ^3He . The implications of the droplet flow model are that (1) the exchange of heat and polarization in the radial direction is perfect, (2) the contribution of the dilute phase to the energy and magnetic moment of the liquid in the exchanger is negligible and (3) spin diffusion and thermal conduction are determined by the concentrated phase. It has also been assumed that relaxation limits the polarization to the region where the susceptibilities χ_{3c} and χ_{3d} are constant and that the temperature is low enough for the concentrated and dilute phase to be degenerate. A detailed derivation is given in Ref. 49. The time evolution of P_{3c} is given by:

$$\frac{\partial P_{3c}}{\partial t} = D_s \frac{\partial^2 (P_{3c} - P_{3c}^e)}{\partial z^2} - \frac{\dot{n}_3(1-\beta)}{n^*} \frac{\partial P_{3c}}{\partial z} \left[\frac{\partial P_{3c}}{\partial z} \right] - \frac{P_{3c} - P_{3c}^e}{T_1} \quad (\text{A1})$$

where D_s is the spin diffusion coefficient of $^3\text{He}_c$, \dot{n}_3 the ^3He circulation rate, $\beta = T_c^*/T_d^*$, n^* the number of moles of $^3\text{He}_c$ per length of exchanger, P_{3c}^e the equilibrium polarization of $^3\text{He}_c$ and T_1 the relaxation time of $^3\text{He}_c$.

An equation for the time evolution of T can be obtained by realizing that the conserved thermodynamic potential for the saturated ^3He - ^4He mixture in the exchanger is given by $\varepsilon = \sum n_i s_i T + \sum n_i (\mu_i + m_i g z)$ where i denotes $^4\text{He}_d$, $^3\text{He}_{d1}$, $^3\text{He}_{d2}$, $^3\text{He}_{c1}$ and $^3\text{He}_{c2}$, ε is an energy density and n_i a molar density. ε obeys the continuity equation

$$\frac{\partial \varepsilon}{\partial t} + \bar{\nabla} \cdot \bar{J}_\varepsilon = 0 \quad (\text{A2})$$

which can be written as

$$\frac{\partial \varepsilon}{\partial t} = -\bar{\nabla} \cdot \bar{J}_q - \sum \bar{\nabla}(\mu_i + m_i g z) \cdot \bar{J}_i + \sum (\mu_i + m_i g z) \frac{\partial n_i}{\partial t} \quad (\text{A3})$$

if we neglect the kinetic energy contribution to ε and assume that $n_{3c} = n_{3c1} + n_{3c2}$, $n_{3d} = n_{3d1} + n_{3d2}$ and n_4 are constant. We remark that the time derivative on the right hand side is due to chemical reactions (or magnetic relaxation) only and that the time derivative on the left hand side arises from all contributions on the right hand. \bar{J}_q is the heat current density due to the thermal conductivity along the exchanger and the entropy convection because of the circulation of dilute and concentrated phase.

Integration of Eq. (A3) over the cross-section of the exchanger leads to:

$$\begin{aligned}
 n^x \gamma_{3c} \frac{\partial T^2}{\partial t} + 2n^x RT_c^* (P_{3c} - P_{3c}^e) \frac{\partial P_{3c}}{\partial t} \\
 = n_3 (\gamma_{3d} - \gamma_{3c}) \frac{\partial T^2}{\partial z} + \sigma \kappa \frac{\partial}{\partial z} \left(\frac{1}{T^2} \frac{\partial T^2}{\partial z} \right) + \frac{2n_3 (1 - x_{ds}) g (m_4 - \rho_{3c} v_{40})}{x_{ds}} \\
 + 2n^x D_s RT_c^* \left(\frac{\partial (P_{3c} - P_{3c}^e)}{\partial z} \right)^2 + \frac{2n^x RT_c^*}{T_1} (P_{3c} - P_{3c}^e)^2 \quad (A4)
 \end{aligned}$$

where γ_{3c} and γ_{3d} are the coefficients of the linear specific heat dependence on T per mole of ^3He in the concentrated and dilute phase, R is the gas constant, σ the cross-section of the exchanger, κ/T the thermal conductivity of $^3\text{He}_c$, x_{ds} the saturation concentration of the dilute phase, g the gravity constant, m_4 the molar mass of ^4He , ρ_{3c} the molar density of $^3\text{He}_c$ and v_{40} the molar volume of pure ^4He . The left hand side of Eq. (A4) follows directly from the left hand side of Eq. (A3). The derivative $\partial P_{3c}/\partial t$ in the second term on the left hand side of Eq. (A4) is to be interpreted as the solution of Eq. (A1). The first term on the right hand side follows partly from the entropy current due to the counterflow of dilute and concentrated phase. The second term is the thermal conduction along the exchanger. The term $\sum \bar{V}(\mu_i + m_i gz) \cdot \bar{J}_i$ in Eq. (A3) contributes to the entropy convection term in Eq. (A4) and gives rise to the third (change of chemical potential of the ^4He in the dilute droplets falling in the gravitational field) and the fourth term (dissipation due to diffusion) in Eq. (A4). The fifth term in Eq. (A4) follows from the last term in Eq. (A3) and describes the dissipation due to the relaxation of the out of equilibrium polarization. We remark that Eq. (A4) with the left hand side equal to zero and without the fourth and the fifth term on the right hand side has been derived in Ref. 25, except for a small error in the first term.⁴⁹ Those equations have to be supplemented with appropriate boundary conditions in the mixing and demixing chamber. We have solved them numerically.⁴⁹ The solutions show: (1) the hand waving arguments made in Sec. IIIB to derive Eq. (19) are justified and (2) the spin diffusion may cause relatively large temperature gradients close to and maybe inside the mixing chamber (see the discussion on systematic errors in Sec. VC).

mass

REFERENCES

1. M. T. Béal-Monod and E. Daniel, *Phys. Rev. B* 27, 4467 (1984).
2. D. Vollhardt, *Rev. Mod. Phys.* 56, 99 (1984).
3. A. Georges, G. Kotliar, W. Krauth, and M. Rozenberg, *Rev. Mod. Phys.* 68, 13 (1996).
4. B. Castaing and P. Nozières, *J. Phys. (Paris)* 40, 257 (1979).

5. F. Laloë and C. Lhuillier, *J. Phys. (Paris)* **40**, 239 (1979).
6. G. Tastevin, P. J. Nacher, L. Wiesenfeld, M. Leduc, and F. Laloë, *J. Phys. (Paris)* **49**, 1 (1988).
7. S. A. J. Wieggers, C. C. Kranenburg, T. Hata, R. Jochemsen, and G. Frossati, *Europhys. Lett.* **10**, 477 (1989).
8. S. A. J. Wieggers, P. E. Wolf, and L. Puech, *Phys. Rev. Lett.* **66**, 2895 (1991).
9. D. Candela, M. E. Hayden, and P. J. Nacher, *Phys. Rev. Lett.* **73**, 2587 (1994).
10. P. J. Nacher and E. Stoltz, *J. Low Temp. Phys.* **101**, 311 (1995).
11. P. J. Nacher, I. Shinkoda, P. Schleger, and W. N. Hardy, *Phys. Rev. Lett.* **67**, 839 (1991).
12. A. Rodrigues and G. Vermeulen, *J. Low Temp. Phys.* **101**, 151 (1995).
13. D. S. Greywall, *Phys. Rev. B* **29**, 4933 (1984).
14. A. S. Sachrajda, D. F. Brewer, and W. S. Truscott, *J. Low Temp. Phys.* **56**, 617 (1984).
15. G. Bonfait, L. Puech, A. S. Greenberg, G. Eska, B. Castaing, and D. Thoulouze, *Phys. Rev. Lett.* **53**, 1092 (1984).
16. G. Tastevin, *Physica B* **194-196**, 911 (1994).
17. G. Bonfait, L. Puech, W. P. Halperin, and B. Castaing, *Europhys. Lett.* **3**, 489 (1987).
18. A. I. Ahonen, M. A. Paalanen, R. C. Richardson, and Y. Takano, *J. Low Temp. Phys.* **25**, 733 (1976).
19. G. E. Watson, J. D. Reppy, and R. C. Richardson, *Phys. Rev.* **188**, 384 (1969).
20. A. Ghazian and E. Varoquaux, *Ann. Phys. Fr.* **4**, 239 (1979).
21. F. Dalfovo and S. Stringari, *J. Low Temp. Phys.* **71**, 311 (1988).
22. L. P. Roobol, G. Frossati, K. S. Bedell, and A. E. Meyerovich, *J. Low Temp. Phys.* **100**, 339 (1995).
23. P. Remeijer, Ph.D. Thesis, Rijksuniversiteit Leiden, Leiden (1966).
24. W. Griffioen, H. W. Jentink, and R. de Bruyn Ouboter, *Physica* **141B**, 137 (1986).
25. W. van Haeringen, F. A. Staas, and J. A. Geurst, *Philips J. Res.* **34**, 127 (1979).
26. G. A. Vermeulen, A. Schuhl, F. B. Rasmussen, J. Joffrin, and M. Chapellier, *J. Low Temp. Phys.* **76**, 43 (1989).
27. J. Landau, J. T. Tough, N. R. Brubaker, and D. O. Edwards, *Rev. Sci. Instrum.* **41**, 444 (1970).
28. D. S. Greywall and P. A. Busch, *J. Low Temp. Phys.* **46**, 451 (1982).
29. J. Landau, J. T. Tough, N. R. Brubaker, and D. O. Edwards, *Phys. Rev. A* **2**, 2472 (1970).
30. H. Ramm, P. Pedroni, J. R. Thompson, and H. Meyer, *J. Low Temp. Phys.* **2**, 539 (1970).
31. H. H. Hensley, Y. Lee, P. Hamot, T. Mizusaki, and W. P. Halperin, *J. Low Temp. Phys.* **90**, 149 (1993).
32. A. C. Anderson, D. O. Edwards, W. R. Roach, R. E. Sarwinski, and J. C. Wheatley, *Phys. Rev. Lett.* **18**, 367 (1966).
33. P. J. Nacher, I. Shinkoda, P. Schleger, and W. N. Hardy, *J. Low Temp. Phys.* **84**, 159 (1991).
34. D. S. Greywall, *Phys. Rev. B* **27**, 2747 (1983); D. S. Greywall, *Phys. Rev. B* **33**, 7520 (1986).
35. S. Yorozu, M. Hiroi, H. Fukuyama, H. Akimoto, H. Ishimoto, and S. Ogawa, *Phys. Rev. B* **45**, 12942 (1992).
36. E. Polturak and R. Rosenbaum, *J. Low Temp. Phys.* **43**, 477 (1981).
37. H. C. Chocholacs, R. M. Mueller, J. R. Owers-Bradley, Ch. Buchal, and M. Kubota, *Proceedings of the 17th International Conference on Low Temperature Physics*, U. Eckern, A. Schmid, W. Weber, and H. Wuhl (eds.), North-Holland, Amsterdam (1984), p. 1247.
38. H. Ishimoto, H. Fukuyama, T. Fukuda, T. Tazaki, and S. Ogawa, *Phys. Rev. B* **38**, 6422 (1988).
39. J. R. Owers-Bradley, D. R. Wightman, A. Child, A. Bedford, and R. M. Bowley, *J. Low Temp. Phys.* **88**, 221 (1992).
40. E. D. Nelson and W. J. Mullin, *J. Low Temp. Phys.* **97**, 251 (1994).
41. A. Rodrigues and G. Vermeulen, *Czech. J. of Phys.* **46-Suppl.**, 241 (1996).
42. D. Vollhardt and P. Wölffe, *Phys. Rev. Lett.* **47**, 190 (1981).
43. K. S. Bedell and D. E. Meltzer, *Phys. Lett.* **106A**, 312 (1984).
44. D. O. Edwards and M. S. Pettersen, *J. Low Temp. Phys.* **87**, 473 (1992).

1996

45. C. A. M. Castelijns, J. G. M. Kuerten, A. T. A. M. de Waele, and H. M. Gijsman, *Phys. Rev. B* 32, 2870 (1985).
46. J. G. M. Kuerten, C. A. M. Castelijns, A. T. ~~M.~~ M. de Waele, and H. M. Gijsman, *Phys. Rev. Lett.* 56, 2288 (1986).
47. J. A. Geurst, F. A. Staas, and W. van Haeringen, *Phys. Lett.* 55A, 251 (1975).
48. I. A. Fomin and G. A. Vermeulen, *J. Low Temp. Phys.* ~~to be published~~.
49. A. Rodrigues, Ph.D. Thesis, Université Joseph Fourier, Grenoble (1996).

A

106, 133 (1997)
1996

Ⓒ Ⓒ Ⓒ Ⓒ Ⓒ Ⓒ Ⓒ Ⓒ Ⓒ Ⓒ

CENTRE DE RECHERCHES SUR LES TRES BASSES TEMPERATURES

Associé à l'Université Joseph Fourier de Grenoble

Siège : 25 Avenue des Martyrs

Adresse Postale :

Boîte postale 166
38042 GRENOBLE Cedex 9
France

Gerard Vermeulen

Tél. 04.76.88.12.61

Télex 320254 Téléfax 76.87.50.60

Bitnet : <gvermeul@labs.polycnrs-gre.fr>

Doreen M. Sauleek

International Centre for Theoretical Physics

P.O. Box 586,

Strada Costiera 11

I-34100 Trieste

Italy

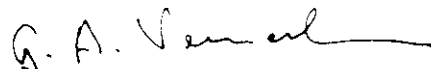
Grenoble, le 19-6-97

Mrs. Sauleek,

inclosed you'll find the proofs of a paper to be published in JLTP. Presently, I am not able to write lecture notes or overhead sheets because of a broken thumb. Anyhow, the paper is nearly a review paper and will be sufficiently clear, I hope. I will bring copies of the overhead sheets too.

By the way, how much time is scheduled for a lecture? and for what kind of audience?

Sincerely yours,



Gerard Vermeulen